2024, 21(6): 1960-1982
https://doi.org/10.21123/bsj.2023.8188
P-ISSN: 2078-8665 - E-ISSN: 2411-7986
Baghdad Science Journal

Synthesis, Characterization, Thermal Analysis Study and Antioxidant Activity for Some Metal Ions Cr (III), Fe (III), Mn (II) and Pd(II) Complexes with Azo Dye Derived from *p*-methyl-2-hydroxybenzaldehyde

Adhraa Ghazi Abdulrazzaq* *, *Abbas Ali Salih Al-Hamdani

Department of Chemistry, College of Science for Women, University of Baghdad, Baghdad, Iraq.
*Corresponding Author.

Received 01/12/2022, Revised 01/04/2023, Accepted 03/04/2023, Published Online First 20/11/2023, Published 1/6/2024

Abstract

A new Azo Dye ligand HL was 4-((3-formyl-2-hydroxyphenyl)diazenyl)-N-(5-methylisoxazol-3-yl)benzenesulfonamide,this synthesized ligand was used for complexation with different metal ions like Cr(III), Fe(III), Mn(II) and Pd(II) by using a molar ratio of ligand: metalas 1:1. Resulted compounds were characterized by NMR (^{1}H and ^{13}C), UV–vis spectroscopy, TGA, DSC, FT-IR, MS, elemental analysis, magnetic moment and molar conductivity studies. The results showed that the geometrical structural were octahedral geometries for the Cr(III), Mn(II) and Fe(III) complexes, square planer for Pd(II) complex. The antioxidant activities of the prepared compounds were assessed by using 1.1-diphenyl-2-picrylhydrazyl as the free radical, and the results showed that the complex azo dye were found to possess potent antioxidant activity. The structure–activity relationship of the ligand and its complexes indicates that the presence of electron-donating moieties, such as Cr(III), Mn(II) and Fe(III), in the chemical structure increases the antioxidant activity, whereas the Pd(II) complexes diminished the antioxidant activity, indicating the superior activity of the hydroxyl radical (OH·) over the superoxide radical.

Keywords: antioxidant, azo dye, 2- hydroxyl benzaldehyde derivative, Mass spectroscopy, Thermal analysis.

Introduction

Azo group N=N contributes in the brilliant color of its compounds in vis-area in addition to its sensitivity toward pH changes which can be strong reason of their usage as colorant for tissues and indications in analytical chemistry [1-4]. Azo compounds display geometrical isomerism when exposed to light, trans- isomers are stable and converts into cis-isomer when exposed to light. Such operation called photochromic when completely conversion occurs[5]. When this operation is accompanied with high differentiation in dipole moment, making these substances of high storage optical data [6]. Azo complexes such as azo-quinoline, display nonlinear optical features, such features occupy important role in optical data storage and telicomunications[7-9]. Azo species had

numerous interests as indicators to extract and identify tiny amounts of metal ions in various samples [10-12]. Azo-complexes have been studied intensively because of their important features and applications such as catalysts, antimicrobial, erosion inhibitors and anticancer [13-15]. Azo-complexes that derived from sulfamethoxazole and pyrazole[16, 17] display unique activities against tuberculosis. Azo compounds such as ruthenium complex, which is derived from quinoline, shows anticancer activity because of their role in photodynamic therapy at long wavelengths [18, 19]. Azo-complexes are also used as photo sensors in double -photon photodynamic therapy to cure cancer because of their lower toxicity in dark and high tendency to produce active O-species in addition to their ability to absorb di-photon [20, 21]. The acidic features of π-orbits of N-heterocycles that involved in azo entities provide additional stability for various oxidation states of metal ions. Large amounts of azo-dyes are added to food products to enhance the appearance and food features [22, 23]. Azo complexes especially Cr (III) complex with acidic dyes shows many usages in toners and dying for skin and hair [24]. According to their large industrial applications such as medicinal and spectroscopic-analysis, we aimed to prepare new series of azo-complexes. By the reaction between azo-compound and each of the next metal ions (Cr (III), Fe (III), Mn (II) and Pd (II)).Then using many techniques to identify the formation of such complexes.

Materials and Methods

Materials have supplied from the trading suppliers, (SigmaAldrich, Merck, and others). The auto vector model EA/3000, singleV3O, has been employed to achieve (C-H-N-Sando). Mineral-ions have determined as M-O employing a gravimetric-approaches. Molar-conductivity has been estimated employing Conduct meter W-T-W, 25-°C. 1×10^{-3} M. D/M/S/0 has employed as solvent. Mass-spectra for substances have been collected using mass spectrometry (MS) Q-P-50-A-D-I Analysis Shimadzu QP(E170Ev) -2010-Pluss spectrometer. The spectra were analyzed using a Shimadzu UV-1800 UV-visible spectrophotometer. The FT_IR Prestige-21 was used to investigate the Fourier Transform Infrared (FTIR in burker) spectra (ranges between 4000-600 cm^{-1}, shimedzo).

General Approach of Azo-ligand (HL)

Synthesis of (E)-4-((3-formyl-2-hydroxyphenyl)diazenyl)-N-(5-methylisoxazol-3-yl)benzenesulfonamide

Diazotization coupling strategy relied on the synthesis of this ligand at which, (2.05 g, 0.005 mol.) of sulfamethoxazole were dissolved in the mixture of (4 mL HCl 37% with 35 ml distilled water DW). This mixture is allowed to be cooled under temperature up to 5ºC followed by addition of (0.375 g, 0.005 mol.) $NaNO_2$ dissolved in 30 ml of distilled water with continuous stirring under controlled temperature range and avoid any arising in temperature up to 5 ºC for 30 minutes. After 15 minutes, diazotization operation is accomplished resulting in diazonium salt, which in turn reacts with a solution of (0.615 g, 0.005 mole) salicylaldehyde dissolved in 50ml abs. EtOH and 15 mL of 10% NaOH. with cooling and continuous stirring, during the operation, pale brown precipitate is observed which left for 1 hour under 5 ºC. Finally, this precipitate is filtered, washed with distilled water several periods, recrystallized by abs. ethanol and dried in oven at 50 ºC [25].

Synthesis of Metal Complexes

A specific amount of azo-ligand (HL)derivative, which dissolved in abs. EtOH, is added discontinuously with continuous stirring onto a specific amount for each of the following mineral ions: (Cr (III), Fe (III), Mn (II) and Pd(II)) solutions. The formed mixture is heated and refluxed for one hour up to 80 ºC, followed by cooling at room temperature, after 24 hours, a completely precipitation accomplished, scheme 1. Then, solution containing- precipitate is filtered, washed several periods with WD and washed with little amount of cold EtOH. Finally, recrystallization process using abs. EtOH is carried out for the synthesized complexes. The molar ratio of the synthesized complexes was found to be 1:1 M:L.To evaluate the antioxidant activity, a series of

2024, 21(6): 1960-1982
https://doi.org/10.21123/bsj.2023.8188
P-ISSN: 2078-8665 - E-ISSN: 2411-7986
Baghdad Science Journal

standards, penta various concentrated solutions are prepared. 1L of G_A fluid with EtOH (for dilution benefits). 6-ml of 45g-DPPH sol were added onto 100-ul for each G-A-solution 30 minutes.

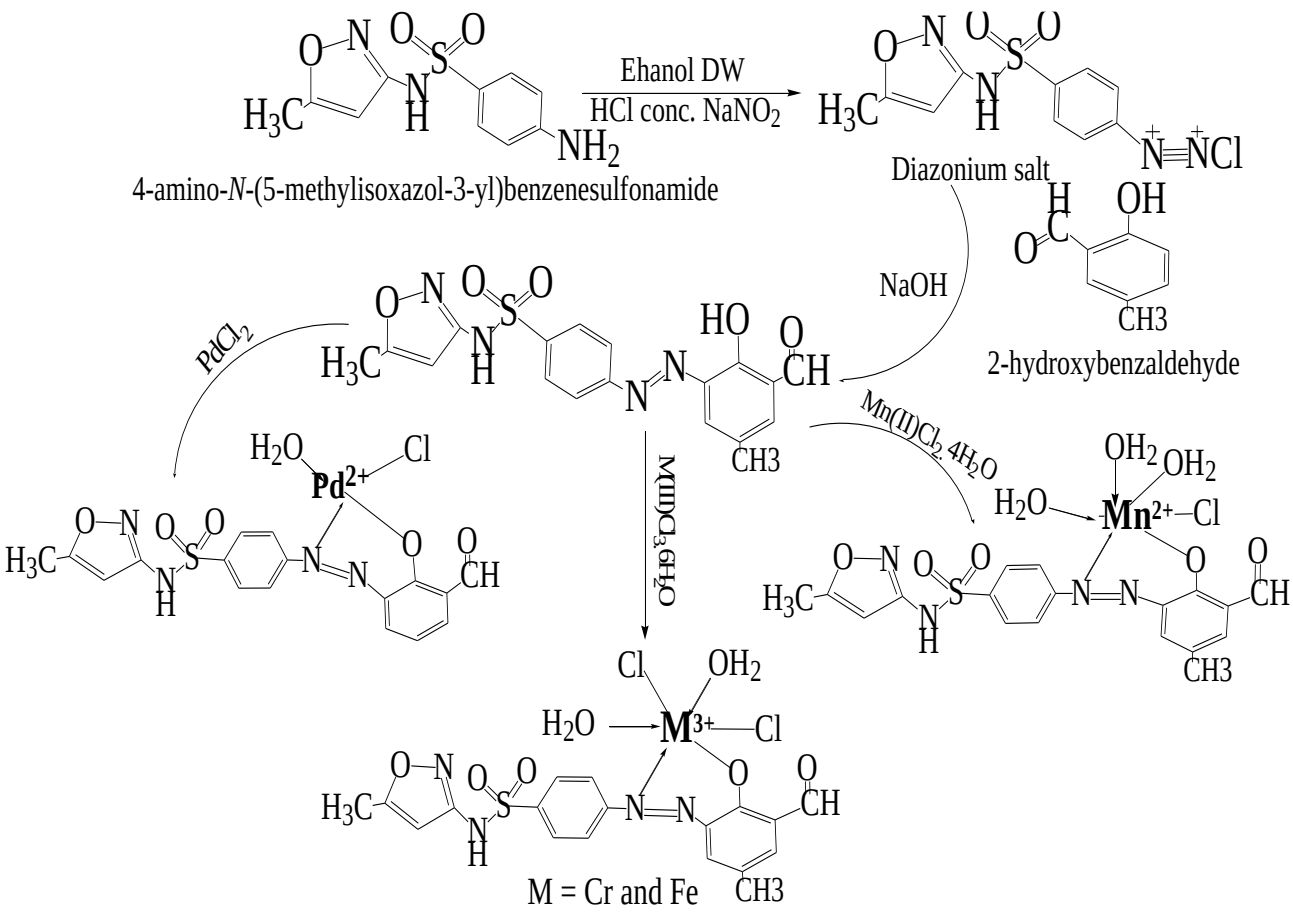

Scheme 1. Azo-ligand (HL) and metal complexes creation pathway

Results and Discussion

Magnetic Nuclear Resonance Spectrum of Ligand (HL):

Magnetic nuclear resonance spectrum of the new azo ligand was studied using dimethyl sulfoxide DMSO-d_6 as solvent and TMS as standard reference. Fig. 1 demonstrates the returns and chemical shifts of these spectra. ^{1}H-NMR spectrum of ligand (HL) demonstrates the following singlet signals as mentioned in (Table 1) 1H of N-H amino group at δ = 11.27 ppm, 1H of H-C=O at δ = 10.75 ppm, 1H of Ar-OH at δ = 10.51 ppm, 1H of C-H (aromatic) besides CH_3 at δ = 5.51 ppm and 3H of CH_3 at δ = 2.60 ppm.In addition, two doublet signals belong to 1H of Ar-H (ortho-H-C=O) and 1H of Ar-H (meta-H-C=O) at δ = (6.92-6.94) ppm and δ = (6.71-6.73) ppm for each of them respectively. Only one multiple signal was detected at δ = (7.58-8.00) ppm. In addition to solvents, signal (DMSO) which observed at δ = (2.51) ppm[26]. ^{13}C-NMR spectrum in Fig. 1, demonstrates the next signals at:30 ppm belongs to (C1), the signals at the range (107-186) ppm belongs to the carbon atoms of aromatic rings (C2-C16). The signal of carbon of aldehyde group C17 was observed at 207 ppm[27].

2024, 21(6): 1960-1982
https://doi.org/10.21123/bsj.2023.8188
P-ISSN: 2078-8665 - E-ISSN: 2411-7986
Baghdad Science Journal

Table 1. ^{1}H-NMR data of azo-ligand (HL).

Compounds	Functional group	(ppm)δ
	N-H	**(11.27, 1H, singlet)**
	H-C=O	**(10.75, 1H, singlet)**
	Ar-OH	**(10.51, 1H, singlet)**
	Ar-H	**(7.58-8.00, 5H, multiplet)**
$C_{18}H_{16}N_4O_5S$	Ar-H (ortho-H-C=O)	**(6.92-6.94,1H,doublate)**
HL	Ar-H (meta-H-C=O)	**(6.71-6.73, 1H, doublate)**
	C-H (aromatic) besides CH_3	**(5.51, 1H, singlet)**
	CH_3	**(2.60, 3H, singlet)**
	DMSO (solvent)	**(2.51)**

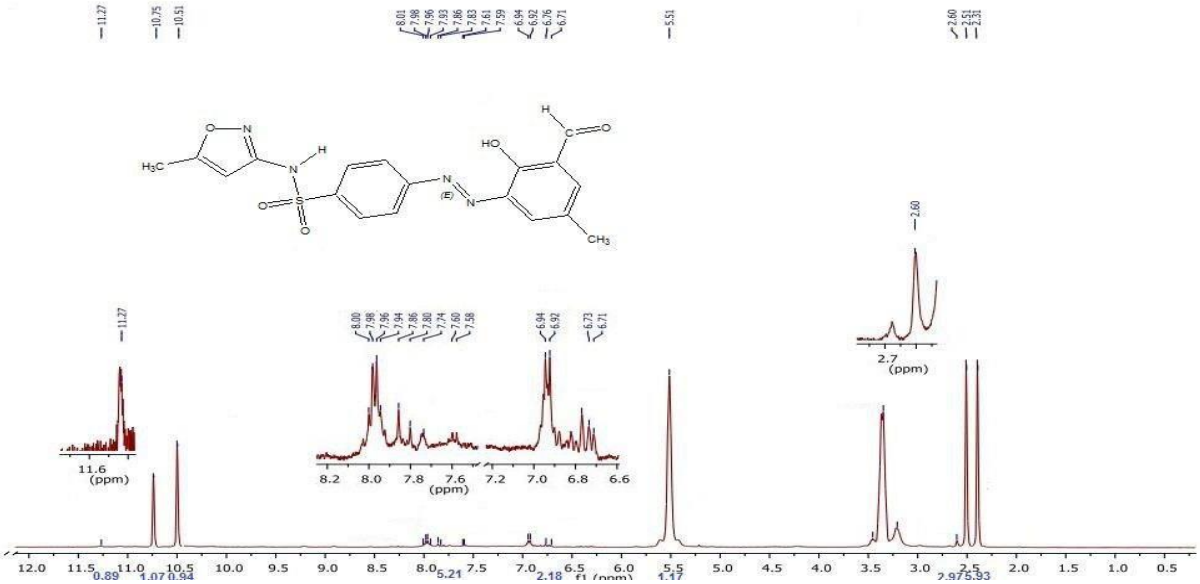

2024, 21(6): 1960-1982
https://doi.org/10.21123/bsj.2023.8188
P-ISSN: 2078-8665 - E-ISSN: 2411-7986
Baghdad Science Journal

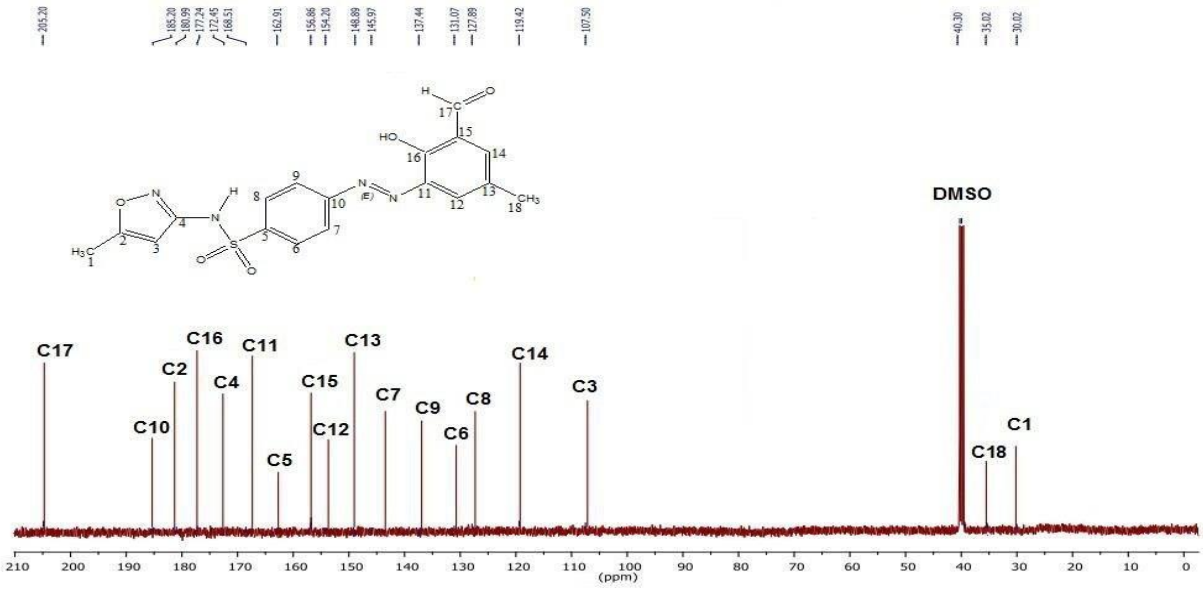

Figure 1.^{1}H-NMR &^{13}C-NMRspectrum of ligand (HL)

Physical and Chemical Properties

Combination of mineral salts with azo-ligand gave azo- complexes Scheme 1. The results of elemental-analysis demonstrates 1:1 M:L stoichiometry for all complexes The elemental-analysis incomes were compatible with theoretical calculated incomes as denoted in Table 2.

Table 2. Some physical properties element microanalysis studies of compounds

Compound M_wt	m-p_°C	Color	Eleme. Micro-ana. Percentageestm. (calc.) C	H.	N.	O.	S	M.	Cl.
$C_{18}H_{16}N_4O_5S$ 386.38	145-147	Pale brown	53.89 (54.00)	3.44 (4.00)	15.55 (14.00)	21.18 (20.00)	8.87 (8.00)	--	--
$C_{18}H_{19}Cl_2CrN_4O_7S$ 544.31	205 d	Brown	37.66 (38.71)	3.59 (3.41)	11.00 (10.04)	21.02 (20.07)	6.18 (5.73)	10.01 (9.32)	12.21 (12.72)
$C_{18}H_{19}Cl_2FeN_4O_7S$ 548.16	200 d	Dark Brown	37.63 (38.43)	3.33 (3.38)	10.98 (9.96)	20.12 (19.93)	6.06 (5.69)	11.01 (9.96)	11.99 (12.63)
$C_{18}H_{21}ClMnN_4O_8S$ 529.81	180 d	Brown	38.73 (39.74)	2.96 (3.86)	11.23 (10.30)	24.01 (23.55)	5.55 (5.88)	11.00 (10.12)	6.07 (6.53)
$C_{18}H_{17}N_4PdO_6SCl$ 545.26	180 d	Dark Brown	3769 (38.68)	2.50 (3.04)	11.81 (10.03)	17.71 (17.19)	6.01 (5.73)	19.21 (18.98)	7.07 (6.36)

d= decompose

UV-Vis Studies of Azo-ligand (HL) and Its Complexes:

UV-Vis spectrum in Fig. 2 displays the electronic transitions of azo-ligand (HL), those transitions as follows: (π →π*), n→π* and (C.T) (L→L). Such transitions can apparently be observed at (261 nm, 38314 cm^{-1}), (352 nm, 28409 cm^{-1}) and (469 nm,21321 cm^{-1}) respectively. The presence of aromatic rings and unsaturated bonds result in (π →π*) transition and the presence of heteroatoms especially unshared electrons cause in n→π* and (C.T) (L→L).[28] Fig. 3 and Table 3 illustrate the electronic transitions of $[Cr(L)(H_2O)_2Cl_2]$ complex at ultra violet region in the range (299 nm, 33444 cm^{-1}) and (362 nm, 27624 cm^{-1}) those absorption bands belong to (π →π*) and (n→π*) electronic transitions respectively. The presence of non-bonding electrons or heteroatoms causes (n→π*) transition, while the presence of unsaturated bonds and aromatic rings causes (π→π*) transition [29]. Moreover, the transitions that happened in metal (d→d), can strongly prove the coordination. Those are as follows;$^4A_2g \rightarrow {}^4T_2g_{(F)}$, $^4A_2g \rightarrow {}^4T_1g_{(F)}$ and $^4A_2g \rightarrow {}^4T_1g_{(P)}$, which observed at (707 nm, 14144 cm^{-1}), (801 nm,12484 cm^{-1}) and (892 nm, 11210

2024, 21(6): 1960-1982
https://doi.org/10.21123/bsj.2023.8188
P-ISSN: 2078-8665 - E-ISSN: 2411-7986
Baghdad Science Journal

cm^{-1}) respectively. Those transitions and magnetic moment (3.87 B.M) can definitely supports octahedral geometry. We can apparently observe the occurrence of coordination in $[Fe(L)(H_2O)_2Cl_2]$ complex in Fig. 4, because of the observed shifting in absorption range of detected transitions at ultra violet region compared to the range of the same transitions in free azoligand to be appeared at (306 nm, 32679 cm^{-1}), (333 nm ,30030 cm^{-1}) and (398 nm,25125 cm^{-1}) . The mentioned wave numbers belong to ($\pi \rightarrow \pi^*$), ($n \rightarrow \pi^*$) and C.T (M→L) transitions respectively. In addition to d-d transitions in the metal itself that denoted as $^1A_1g \rightarrow {}^1T_2g$at (659 nm, 15174 cm^{-1}) and $^1A_1g \rightarrow {}^1T_1g$ at (768 nm, 13020 cm^{-1}). The magnetic moment (5.55 B.M) can definitely supports Octahedral geometry [30,31]. Mn-complexion in Fig. 5 which shows electronic transitions in ultra violet region, those are ($\pi \rightarrow \pi^*$) and ($n \rightarrow \pi^*$) and (C.T) at (337 nm, 29673 cm^{-1}) and (391 nm,25575cm^{-1}) respectively.
Additionally,$^6A_{1g} \rightarrow {}^4A_{1g}$,$^4E_{g(G)}$,$^6A_1 \rightarrow {}^4T_{2g(G)}$and $^6A_1 \rightarrow {}^4T_{1gG)}$(d→d transitions) can clearly observe at (586 nm, 17064 cm^{-1}), (682 nm, 14662 cm^{-1}) and (780 nm, 12820 cm^{-1}) respectively. Those transitions and the magnetic moment [5.71B.M] can definitely supports octahedral geometry [32].As for Pd- complex shown in Fig. 6, the following transitions: $\pi \rightarrow \pi^*$ at (243 nm,41152cm^{-1}), $n \rightarrow \pi^*$ at (318 nm, 31446cm^{-1}) and (C.T) transition at (396 nm, 25252 cm^{-1}) those belong to azo group. In addition to (d→d) transitions that observed at (613 nm, 16313cm^{-1}) and (678 nm, 14749cm^{-1}) the mentioned transition can definitely support square planer geometry of the complex [33]. All the electronic transitions information for the products have displayed in Table 3.

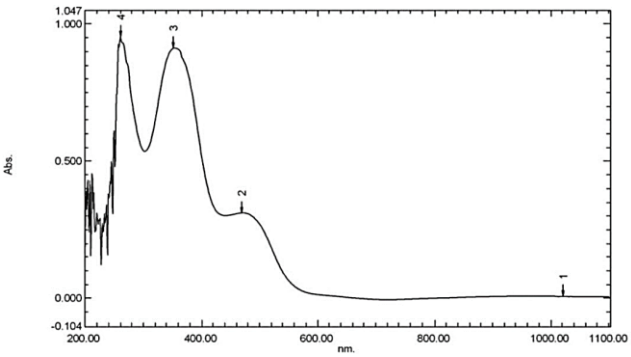

Figure 2. UV-Vis spectrum of ligand (HL)

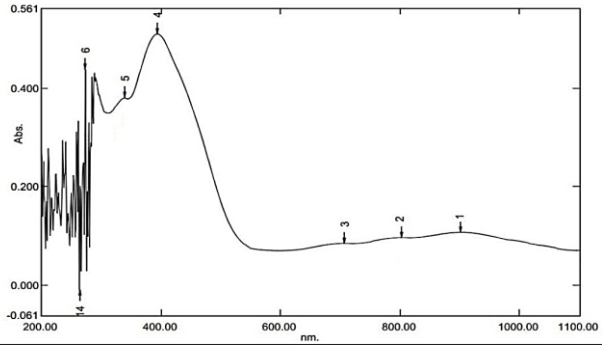

Figure 3. UV-Vis spectrum of Chromium-complex

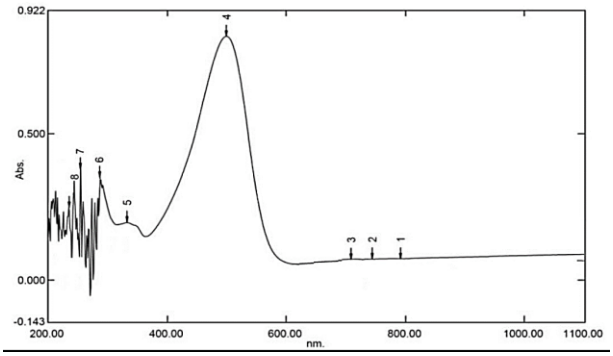

Figure 4. UV-Vis spectrum of Iron-complex

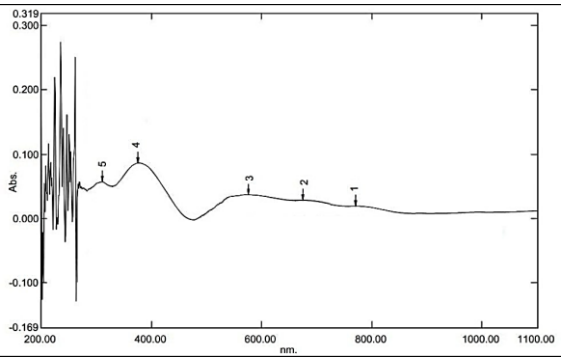

Figure 5. UV-Vis spectrum of Manganese-complex

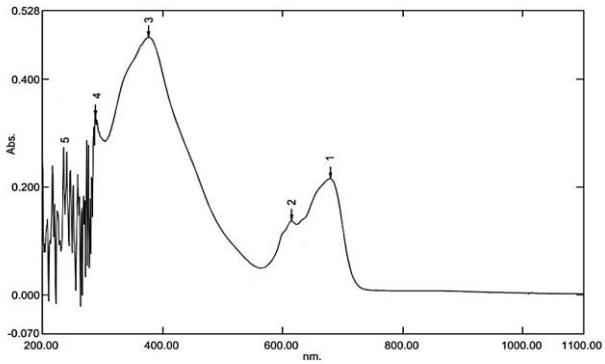

Figure 6. UV-Vis spectrum of Palladium-complex

2024, 21(6): 1960-1982
https://doi.org/10.21123/bsj.2023.8188
P-ISSN: 2078-8665 - E-ISSN: 2411-7986
Baghdad Science Journal

Table 3. UV-Vis spectral incomes of ligand HL and its complexes

Compound	λ_{max} (nm)	υ cm^{-1}	ABS.	ε_{max} L $mol^{-1}cm^{-1}$	Assignment	Λ_m cm^2 $\Omega^{-1}mol^{-1}$	μ_{eff} B.M
$C_{18}H_{16}N_4O_5S$ HL	261	38314	0.951	951	$\pi\rightarrow\pi^*$	-	-
	352	28409	0.911	911	$n\rightarrow\pi^*$		
	469	21321	0.309	309	C.T(L→L)		
	387	25839	0.060	60	$\pi\rightarrow\pi^*$		
	391	25575	0.081	81	$n\rightarrow\pi^*$+C.T		
	586	17064	0.050	50	$^6A_{1g}\rightarrow{}^4A_{1g}$, $^4E_{g(G)}$	13	5.71
	682	14662	0.033	33	$^6A_{1g}\rightarrow{}^4T_{2g(G)}$		
	780	12820	0.020	20	$^6A_{1g}\rightarrow{}^4T_{1gG)}$		
$C_{18}H_{21}ClMnN_4O_8S$(Octahedral)							
	243	41152	0.370	370	$\pi\rightarrow\pi^*$		
$C_{18}H_{17}N_4PdO_6SCl$ (Square planer)	318	31446	0.500	500	$n\rightarrow\pi^*$	17	Diamagnetic
	396	25252	0.100	100	(C.T)		
	613	16313	0.199	199	$^1A_1g\rightarrow{}^1B_1g$		
	678	14749			$^1A_1g\rightarrow{}^1A_2g$		
	299	33444	0.410	410	$\pi\rightarrow\pi^*$		
	362	27624	0.380	380	$n\rightarrow\pi^*$		
	406	24630	0.550	550	(C.T)	16	3.87
$C_{18}H_{19}Cl_2CrN_4O_7S$(Octahedral)	707	14144	0.090	90	$^3T_{1g(F)}\rightarrow{}^3T_{1g(F)}$		
	801	12484	0.100	100	$^3T_{1g(F)}\rightarrow{}^3A_{2g}$		
	892	11210	0.120	120	$^3T_{1g(F)}\rightarrow{}^3T_{1g(P)}$		
	306	32679	0.086	86	$\pi\rightarrow\pi^*$		
$C_{18}H_{19}Cl_2FeN_4O_7S$(Octahedral)	333	30030	0.093	93	$n\rightarrow\pi^*$		
	398	25125	0.123	123	C.T(M→L)	19	5.55
	659	15174	0.022	22	$^1A_1g\rightarrow{}^1T_2g$		
	768	13020	0.026	26	$^1A_1g\rightarrow{}^1T_1g$		

LC/Mss Spectra of the Products:

In Fig. 7 and Scheme 3, we can apparently notice the peak that corresponds the molecular weight of ligand (HL) for the piece$C_{18}H_{16}N_4O_5S$ and its abundance about 20%. In addition to other abundances for the rest of pieces including$C_{10}H_{10}N_3O_3S^+$, $C_4H_5N_2O_3S^+$, $C_7H_6NO_2^+$, $C_6H_6NO^+$ and $C_6H_6N^+$ that corresponded the next abundances: 41%, 58%, 47%, 36% and 50% respectively and detected at (252.11, 161.27, 136.22, 108.21and 92.41) m/z respectively. Mass information of $[Fe(L)(H_2O)_2Cl_2]$ in Fig. 8 and Scheme 4, the peak of $C_{18}H_{18}Cl_2FeN_4O_7S$ can be detected at 562 m/z with relative abundance 12% besides the next patterns $C_{17}H_{12}Cl_2FeN_4O_5S^+$, $C_{17}H_{12}FeN_4O_5S^+$, $C_7H_4FeN_2O_2^+$, $C_6H_5SO_2^+$and $C_4H_5N_2O^+$. Which correspond to (511 m/z, 60%), (440 m/z, 59%), (203 m/z, 55%), (141 m/z, 49%) and (97 m/z, 69%) respectively [34]. Additionally, $[Pd(L)(H_2O)Cl]$ complex in Fig. 9 and Scheme 5, illustrates the next fragments:$C_{18}H_{17}ClN_4O_6PdS$ at 559 m/z with relative abundance 12%, $C_{17}H_{13}N_4O_5PdS^+$, $C_7H_4N_2O_2Pd^+$, $C_{10}H_9N_2O_3S^+$, $C_6H_5SO_2^+$, HN_2Pd^+, $C_7H_5O_2^+$and $C_4H_5N_2O^+$ that corresponded to (491 m/z, 66%), (254 m/z, 49%), (237 m/z, 40%), (141 m/z, 22%), (135 m/z, 36%), (121 m/z, 48%) and (97 m/z, 64%) respectively [35]. $[Cr(L)(H_2O)_2Cl_2]$ complex in Fig. 10 and scheme 6 illustrate the next fragments: $C_{18}H_{19}Cl_2CrN_4O_7S$ at (558 m/z, 14%), $C_{17}H_{12}Cl_2CrN_4O_5S^+$ at (507 m/z, 47%), $C_{17}H_{12}CrN_4O_5S^+$ at (436 m/z, 27%), $C_7H_4CrN_2O_2^+$ at (200 m/z, 46%), $C_6H_5SO_2^+$ at (141 m/z, 45%) and $C_4H_5N_2O^+$ at (97 m/z, 79%) [35]. For $[Mn(L)(H_2O)_3Cl]$ in Fig. 11, Scheme 7 is displayed in detail in (Table 5).

2024, 21(6): 1960-1982
https://doi.org/10.21123/bsj.2023.8188
P-ISSN: 2078-8665 - E-ISSN: 2411-7986
Baghdad Science Journal

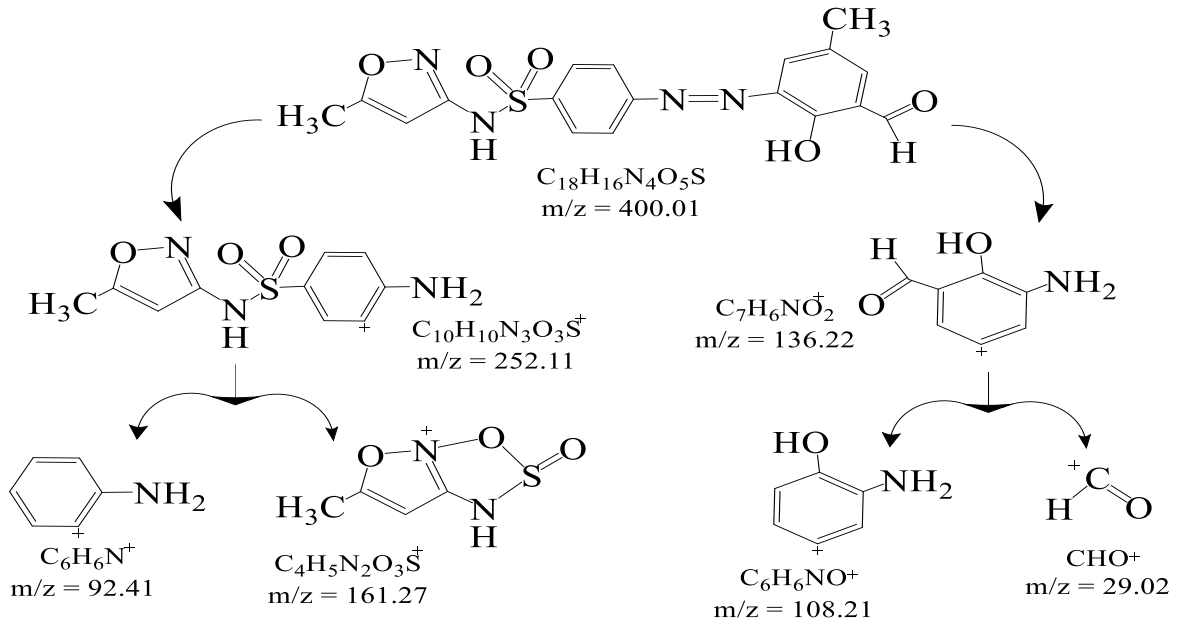

Scheme 3. Partitioning analogues of ligand (HL)

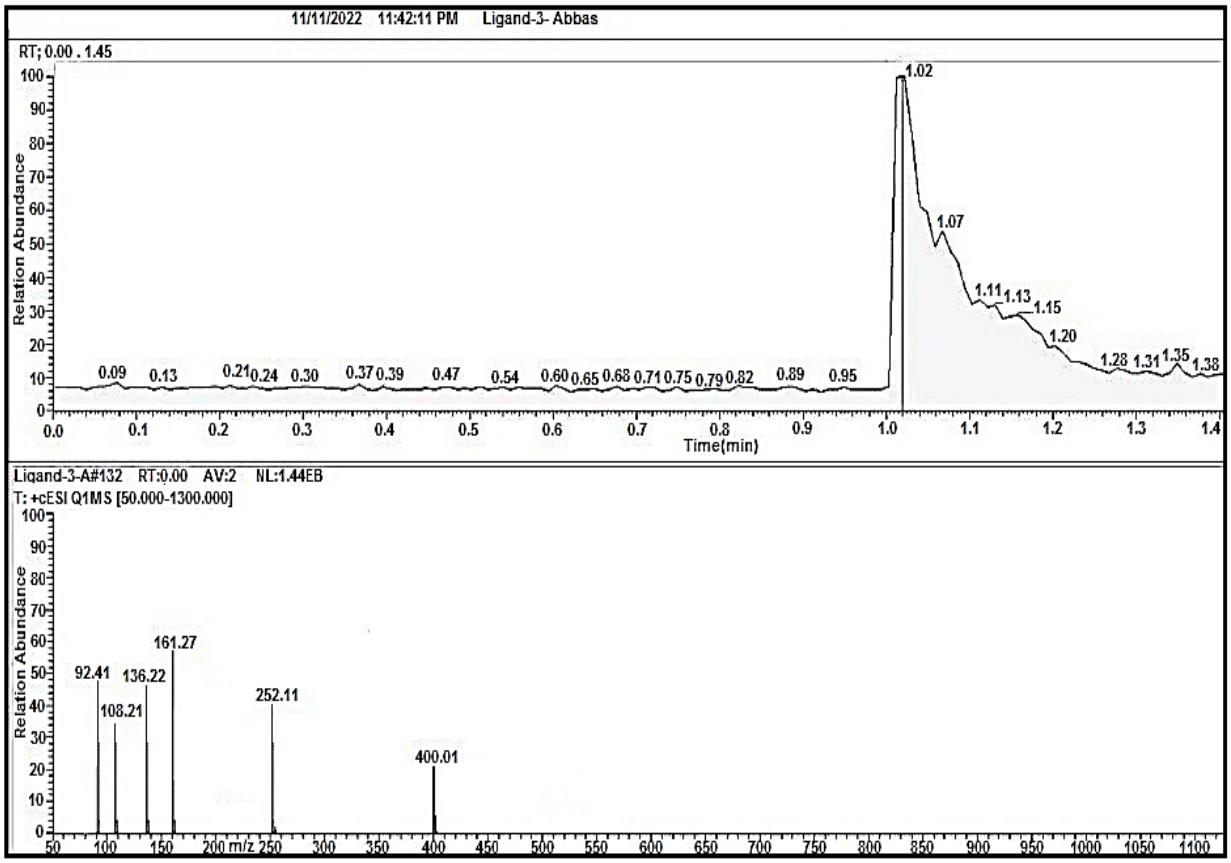

Figure 7. LC-Mass spectrum of ligand (HL)

2024, 21(6): 1960-1982
https://doi.org/10.21123/bsj.2023.8188
P-ISSN: 2078-8665 - E-ISSN: 2411-7986
Baghdad Science Journal

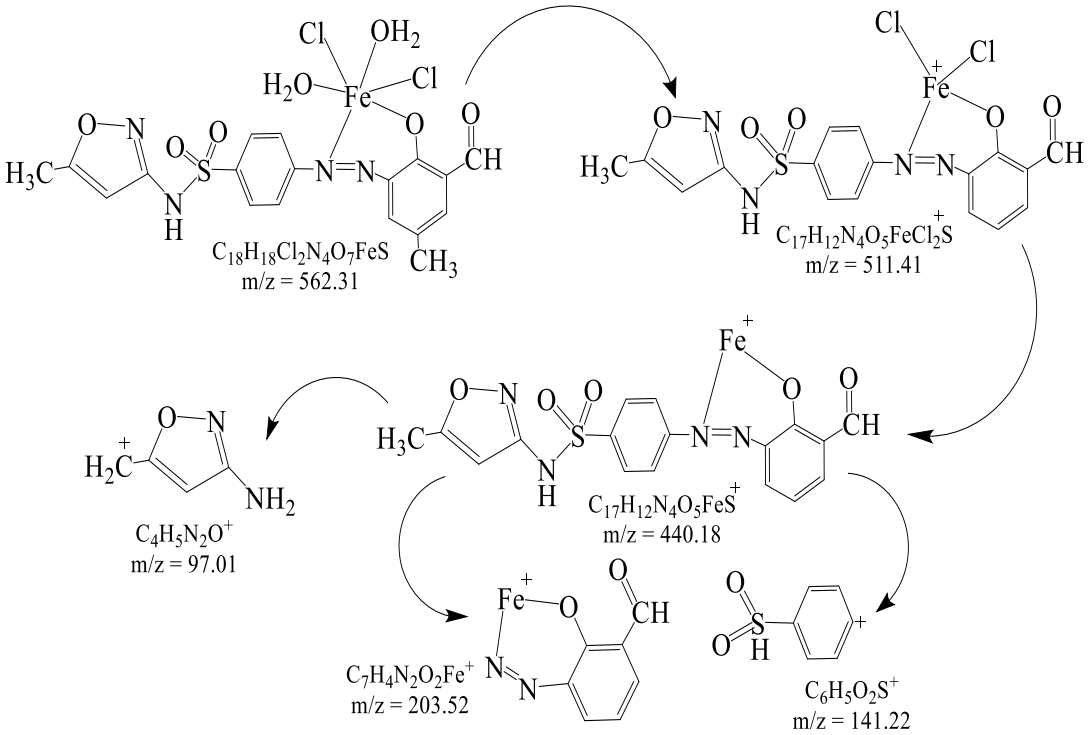

Scheme 4.Partitioning analogues of Iron-complex

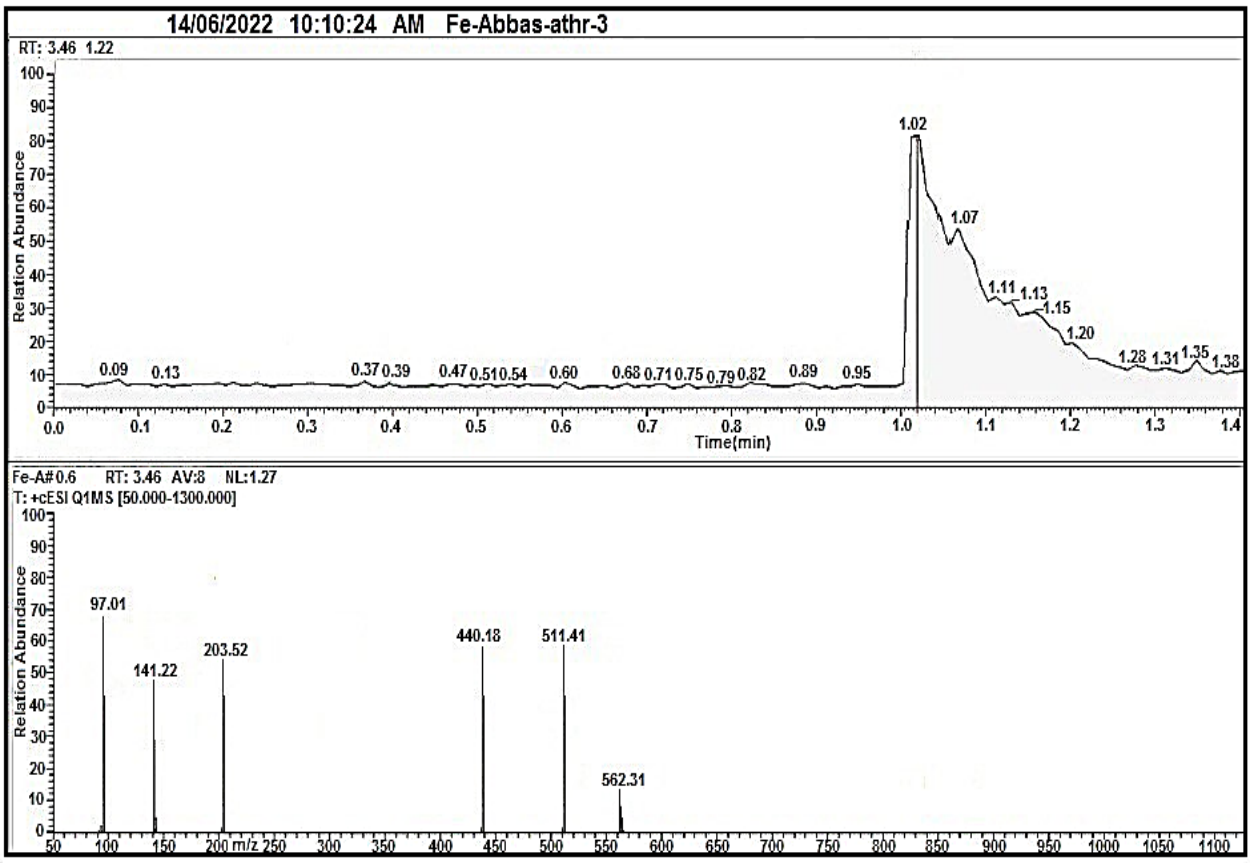

Figure 8. LC-Mass spectrum of Iron-complex

2024, 21(6): 1960-1982
https://doi.org/10.21123/bsj.2023.8188
P-ISSN: 2078-8665 - E-ISSN: 2411-7986
Baghdad Science Journal

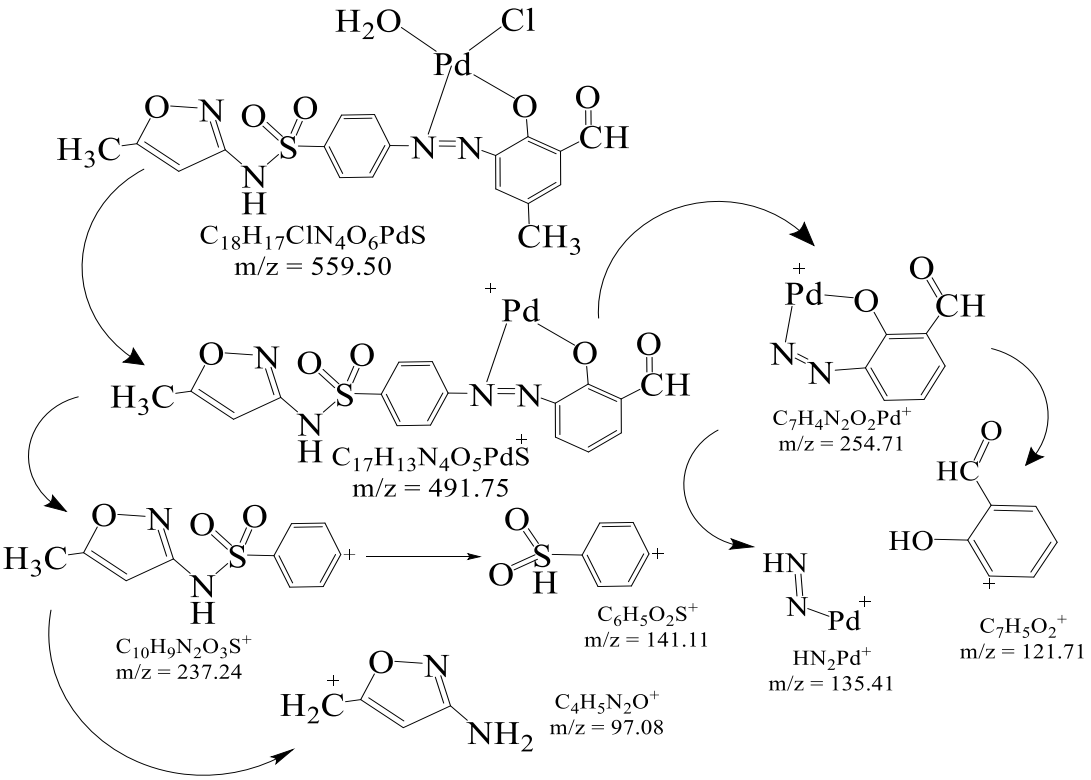

Scheme 5.Partitioning analogues of Palladium-complex

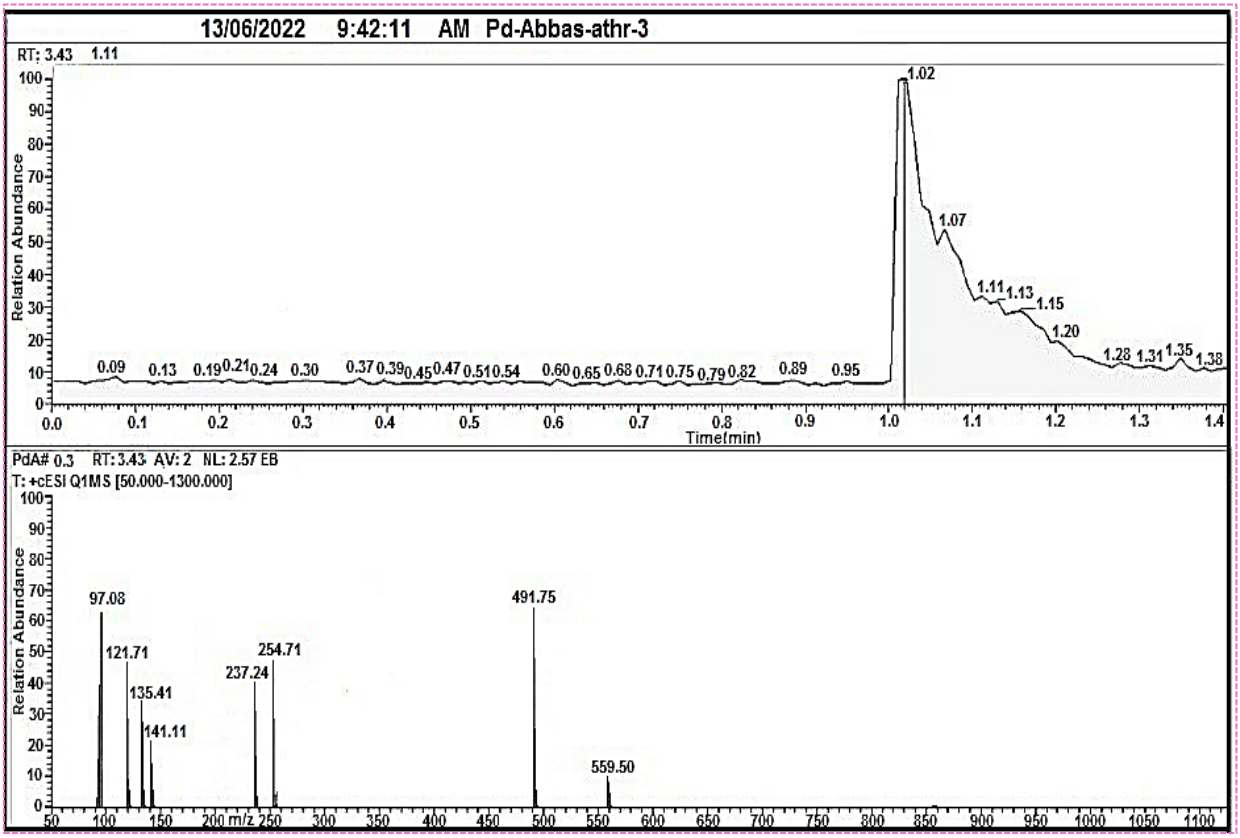

Figure 9. LC-Mass spectrum of Palladium-complex

2024, 21(6): 1960-1982
https://doi.org/10.21123/bsj.2023.8188
P-ISSN: 2078-8665 - E-ISSN: 2411-7986
Baghdad Science Journal

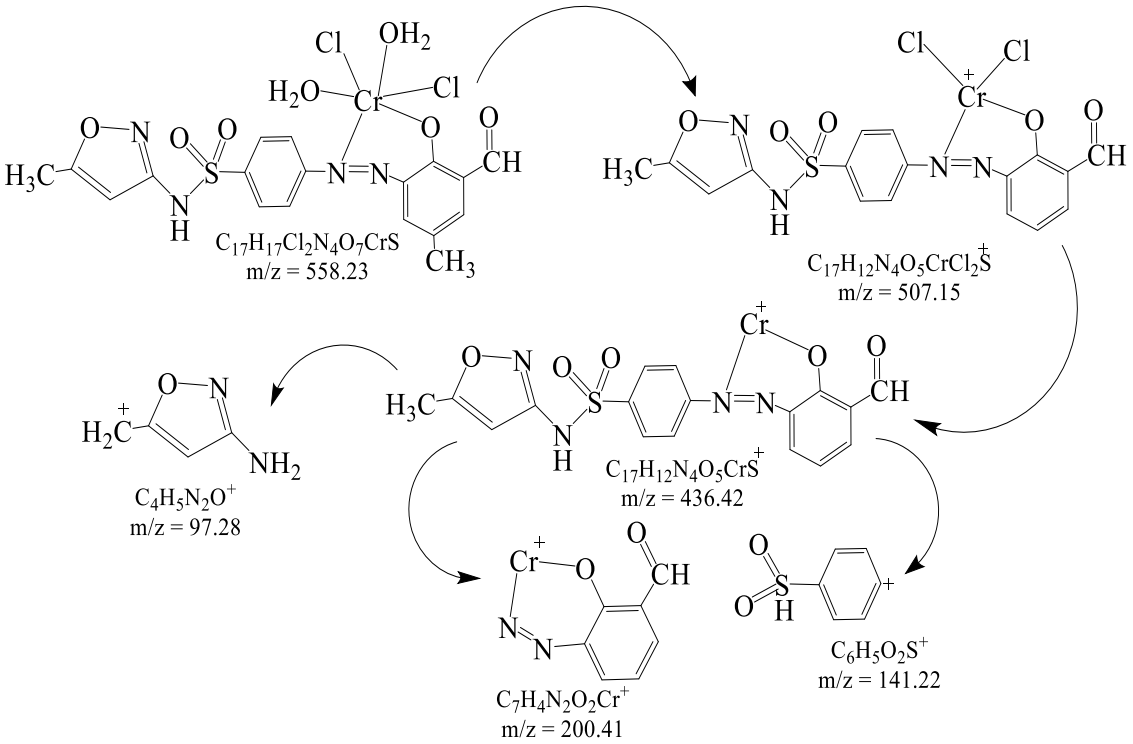

Scheme 6.Partitioning analogues of Chromium-complex

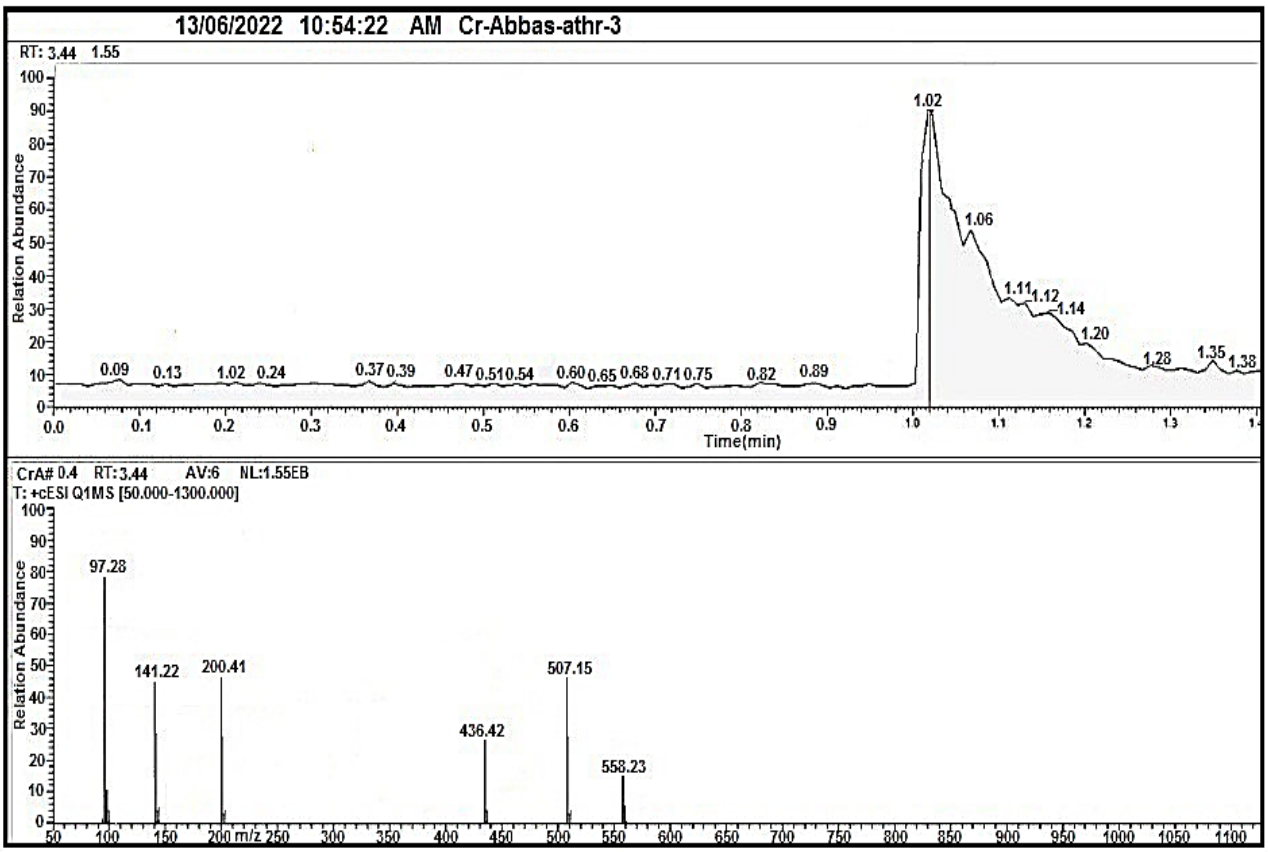

Figure 10. LC-Mass spectrum of Chromium-complex

2024, 21(6): 1960-1982
https://doi.org/10.21123/bsj.2023.8188
P-ISSN: 2078-8665 - E-ISSN: 2411-7986
Baghdad Science Journal

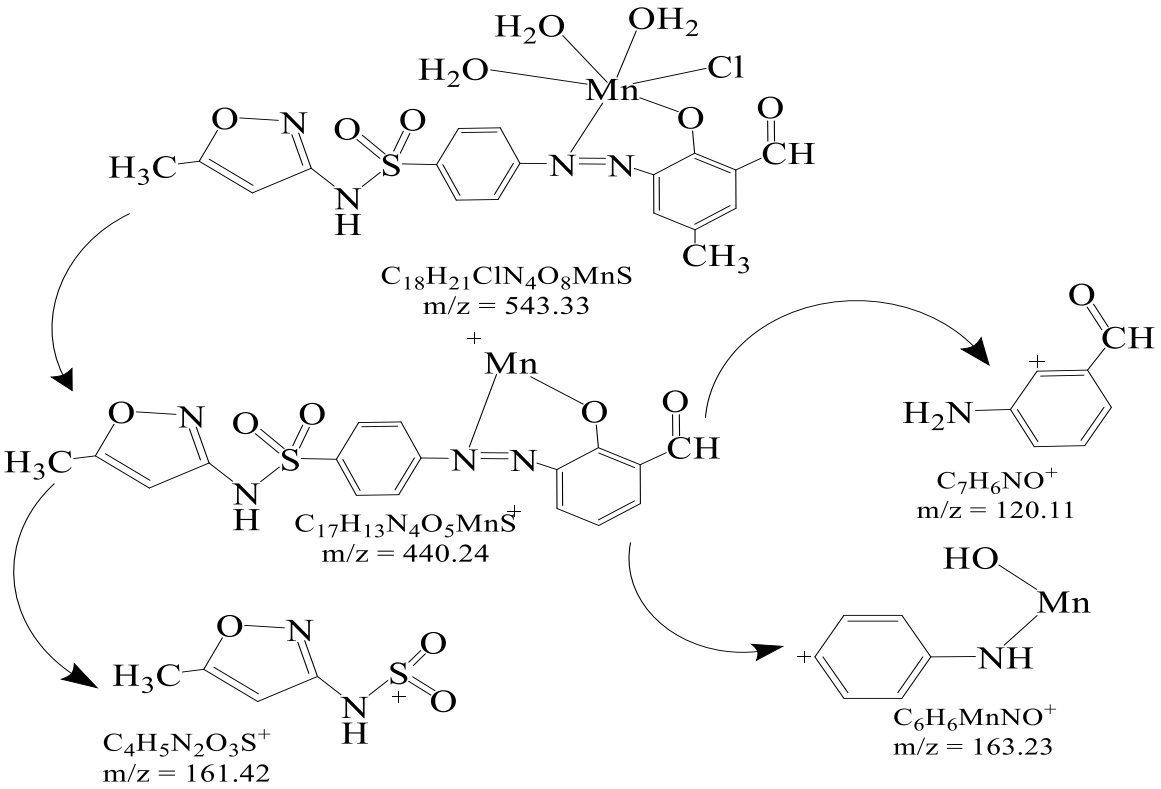

Scheme 7.Partitioning analogues of Manganese-complex

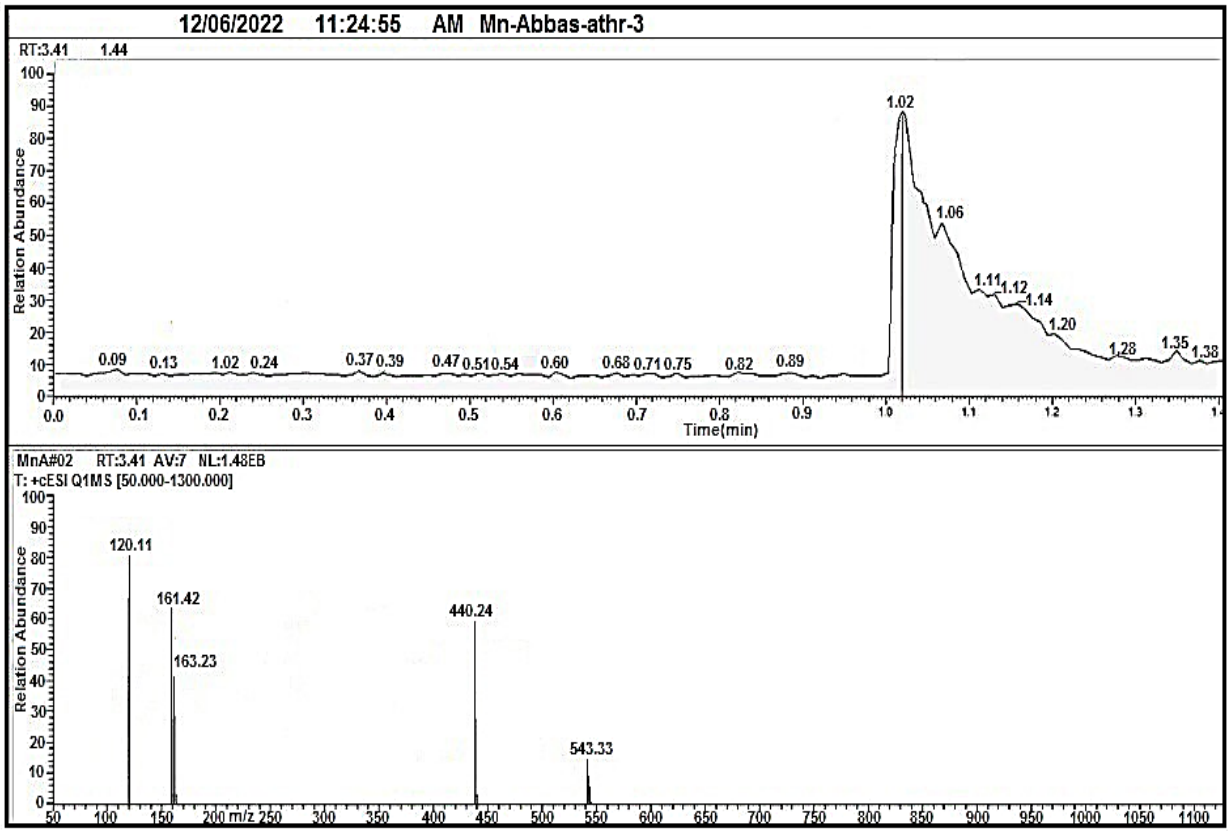

Figure 11. LC-Mass spectrum of Manganese-complex

2024, 21(6): 1960-1982
https://doi.org/10.21123/bsj.2023.8188
P-ISSN: 2078-8665 - E-ISSN: 2411-7986
Baghdad Science Journal

Table 4. LC_Mass informs of ligand (HL) and its complexes

Fragment (HL)	Extract mass	Relative abundance	Fragment Pd-complex	Extract mass	Relative abundance
$C_{18}H_{16}N_4O_5S$	400	20%	$C_{18}H_{17}ClN_4O_6PdS$	559	12%
$C_{10}H_{10}N_3O_3S^+$	252	41%	$C_{17}H_{13}N_4O_5PdS^+$	491	66%
$C_4H_5N_2O_3S^+$	161	58%	$C_7H_4N_2O_2Pd^+$	254	49%
$C_7H_6NO_2^+$	136	47%	$C_{10}H_9N_2O_3S^+$	237	40%
$C_6H_6NO^+$	108	36%	$C_6H_5SO_2^+$	141	22%
$C_6H_6N^+$	92	50%	HN_2Pd^+	135	36%
CHO^+	29	42%	$C_7H_5O_2^+$	121	48%
--	--	--	$C_4H_5N_2O^+$	97	64%
Fragment Cr-complex	**Extract mass**	**Relative abundance**	**Fragment Fe-complex**	**Extract mass**	**Relative abundance**
$C_{18}H_{19}Cl_2CrN_4O_7S$	558	14%	$C_{18}H_{19}Cl_2FeN_4O_7S$	562	12%
$C_{17}H_{12}Cl_2CrN_4O_5S^+$	507	47%	$C_{17}H_{12}Cl_2FeN_4O_5S^+$	511	60%
$C_{17}H_{12}CrN_4O_5S^+$	436	27%	$C_{17}H_{12}FeN_4O_5S^+$	440	59%
$C_7H_4CrN_2O_2^+$	200	46%	$C_7H_4FeN_2O_2^+$	203	55%
$C_6H_5SO_2^+$	141	45%	$C_6H_5SO_2^+$	141	49%
$C_4H_5N_2O^+$	97	79%	$C_4H_5N_2O^+$	97	69%

Table 5. LC_Mass information of manganese complex

Fragment Mn-complex	Extract mass	Relative abundance
$C_{18}H_{21}ClMnN_4O_8S$	543	28%
$C_{17}H_{13}MnN_4O_5S^+$	440	61%
$C_6H_6MnNO^+$	163	42%
$C_4H_5N_2O_3S^+$	161	65%
$C_7H_6NO^+$	120	81%

FT-IR Studies:

The absorption bands that observed in azo-species, Fig. 12, are stretching vibrational modes for each of the next functional groups: (NH) amine, (C-H) aromatic, (C-H) aliphatic, (C-H) aldehydic, (N=N) azo band and (SO_2) at 3477, 3091, 2977, 2891, 1463, 1327, 1086, and 1013 cm^{-1} repectively. In FT-IR spectrum for $[Fe(L)(H_2O)_2Cl_2]$ complex, we can clearly notice the absorption band of coordinated water molecule in the range 3741, 1531 and 653 cm^{-1} that proves the involvement of such group inside the coordination sphere of the complex. Other absorption bands that detected belong to the stretching absorption bands for the next groups : N-H amino group at 3406 cm^{-1}, C-H aromatic at 3052 cm^{-1} , C-H aliphatic at 2964 cm^{-1}, (C-H) aldehydic at 2885 cm^{-1}, N=N at 1463 cm^{-1} and SO_2 group at 1089 and 1002 cm^{-1} .[35] For $[Cr(L)(H_2O)_2Cl_2]$ complex, we can also observe the absorption band of coordinated water molecule at 3445, 1548 and 758 cm^{-1} . and absorption peaks of next functional groups: N-H amino group , C-H aromatic , C-H aliphatic, C-H aldehydic, N=N azo group and SO_2 sulfate group at : 3435 , 3143, 2979, 2827, 1468, 1136 and 1060 cm^{-1} respectively.[36] The FT-IR spectrum of $[Mn(L)(H_2O)_3Cl_2]$ complex displays the same absorption bands that shown in previous complexes. N-H amino group, C-H aromatic, C-H aliphatic, C-H aldehydic, N=N azo group and SO_2 sulfate group at: 3381, 3143, 2979, 2887, 1462, 1088 and 1015 cm^{-1} respectively. Besides the band of coordinated water molecule which in turn observed at 3503, 1543 and 721 cm^{-1}. [37] The FT-IR spectrum of $[Pd(L)(H_2O)Cl]$ [38]complex in Fig. 13, displays the same absorption bands that shown in previous complexes. N-H amino group, C-H aromatic, C-H aliphatic, C-H aldehydic, N=N azo group and SO_2 sulfate group at: 3453, 3036, 2978, 2889, 1487, 1083 and 1008 cm^{-1} respectively. Besides the band of coordinated water molecule which in turn observed at 3509, 1573 and 754 cm^{-1}. All the information data of the complexes have displayed in Table 6.

2024, 21(6): 1960-1982
https://doi.org/10.21123/bsj.2023.8188
P-ISSN: 2078-8665 - E-ISSN: 2411-7986
Baghdad Science Journal

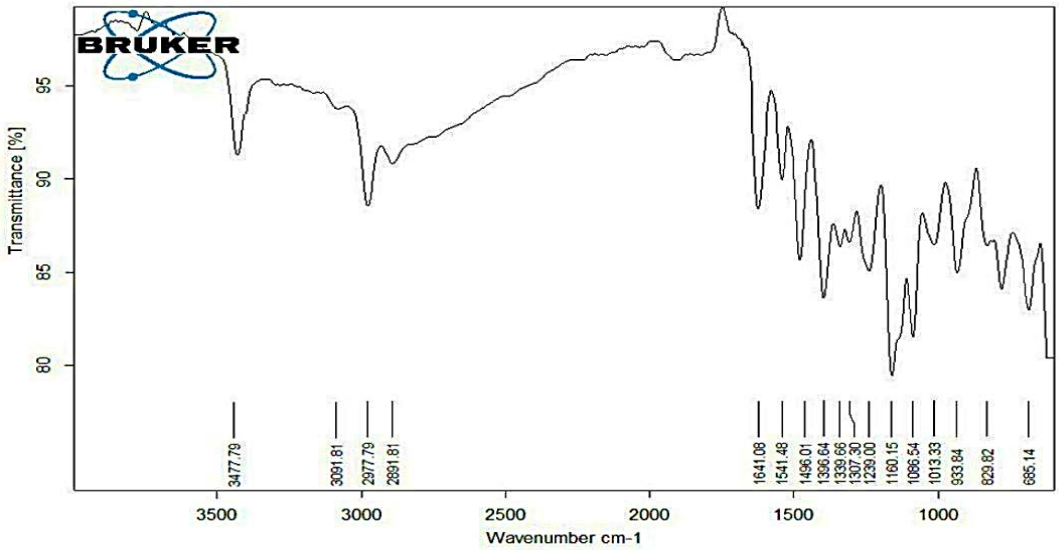

Figure 12. FT-IR spectrum of ligand (HL)

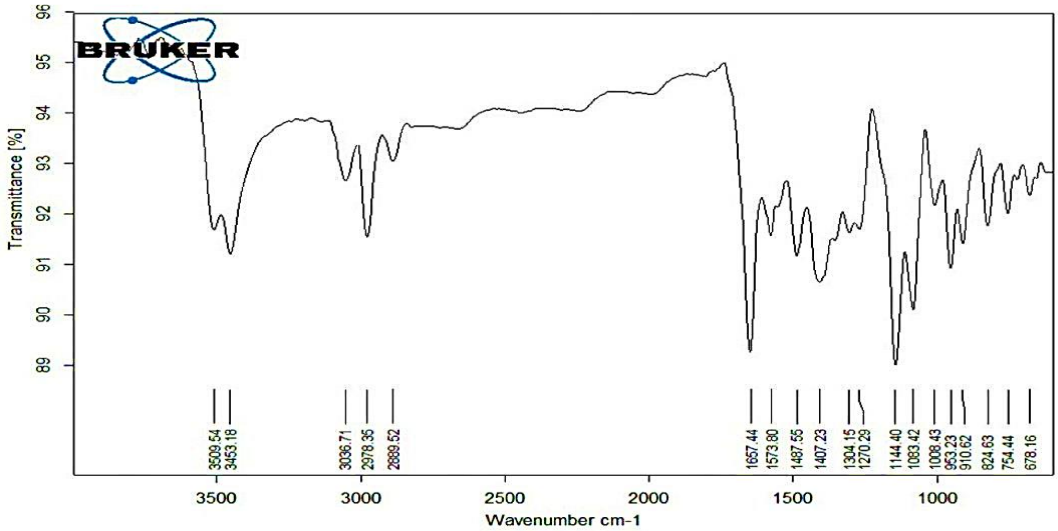

Figure 13. FT-IR spectrum of Palladium-complex

Table 6. FT-IR incomes of azo_former and its complexes

Compound	H_2O aqua	NH amine	C-H aromatic	C-H aliphatic	C-H aldehyde	C=O aldehyde	N=N azo	SO_2	M-N (M-O)	M-Cl
$C_{18}H_{16}N_4O_5S$	--	3477	3091	2977	2891	1641	1463	1086 1013	--	--
$C_{18}H_{21}ClMnN_4O_8S$	3503 1543 721	3481	3143	2979	2887	1642	1462	1088 1015	495 (426)	323
$C_{18}H_{19}Cl_2CrN_4O_7S$	3445 1548 758	3435	3143	2979	2827	1646	1468	1137 1060	510 (451)	315
$C_{18}H_{19}Cl_2FeN_4O_7S$	3741 1531 753	3406	3052	2964	2885	1653	1463	1089 1002	553 (432)	342
$C_{18}H_{17}N_4PdO_6SCl$	3509 1573 754	3453	3036	2978	2889	1657	1487	1083 1008	498 (430)	335

2024, 21(6): 1960-1982
https://doi.org/10.21123/bsj.2023.8188
P-ISSN: 2078-8665 - E-ISSN: 2411-7986
Baghdad Science Journal

Study of Thermogravimetric Analysis for Azo-ligand (HL) and Complexes:

DSC differential scanning calorimetry technique, defined as pyrolysis technique was employed for estimating the amount of absorbed and released heat and for the thermal changes that happened for tested substance. Table 7, shows T_i/ºC, T_f/ºC, heat amount (ΔH) in J/g unit if it was exothermic or endothermic. Pyrolysis studies for Azo-ligand (HL)and its complexes were carried out depending on thermogravimetric analysis curve (TGA) by measuring the changes in masses of the substances under study relative to temperature when these substances obey to controlled thermal program in a specific time. The result curve is considered as thermogravimetric curve, which inform us about thermal stability, reaction rates, chemical structure and the thermal stability of the products as denoted in Table 8. in addition to each pyrolysis step occurred. TGA for the ligand (HL) in Fig. 14 shows a single degradation step at which, the calculated mass loss is 96.683% and the experimental mass loss is 98.542 and the remnant was found to be 1.458. Manganese-complex in Fig. 15, analyzes in two steps as illustrated in the figure that displays the mechanism of its degradation, the critical temperature at which the maximal transformation of the complex occurs and the percentage of theoretical and calculated mass loss. It was found that, the estimated mass loss is 86.540% and the remnant is 13.460% whereas the calculated mass loss is 87.037 % and the remnant is 12.963 % as MnO [39] Fig. 16, for Palladium-complex, displays two degradation steps, the critical temperature at which the maximum mutation of complex carried out and the percentage of theoretical 80.704% and the remnant is 19.296%, and calculated mass loss 80.0535 % and the remnant is 19.9465% as PdO. [40] all the pyrolysis information has shown in Scheme 7.

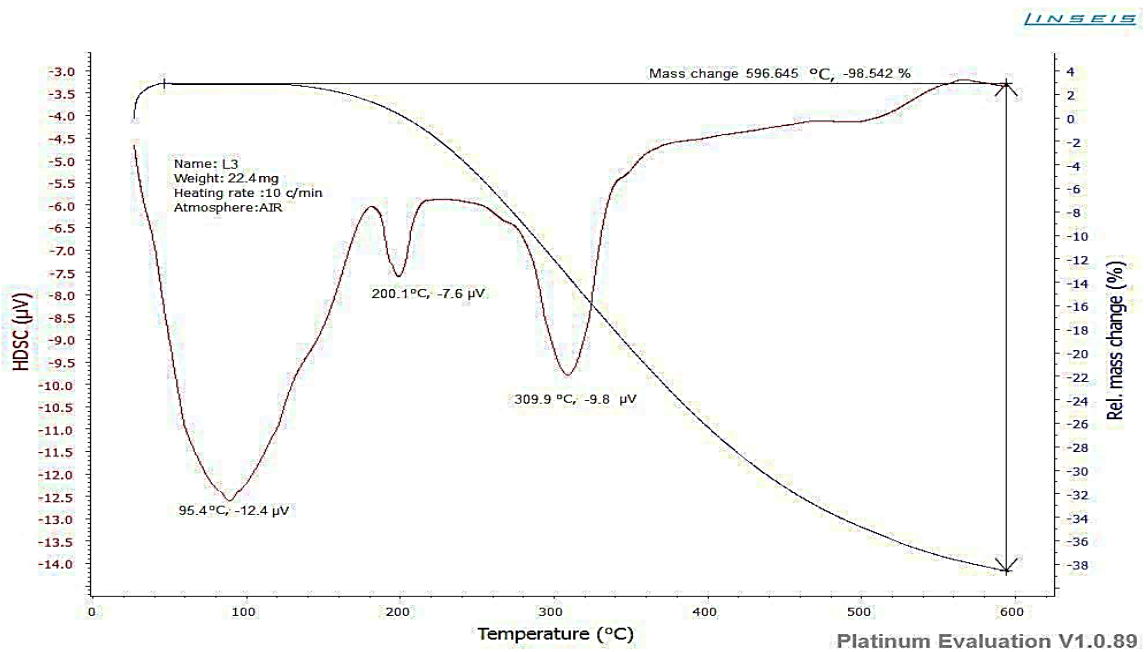

Figure 14. Thermogram of ligand (HL)

2024, 21(6): 1960-1982
https://doi.org/10.21123/bsj.2023.8188
P-ISSN: 2078-8665 - E-ISSN: 2411-7986
Baghdad Science Journal

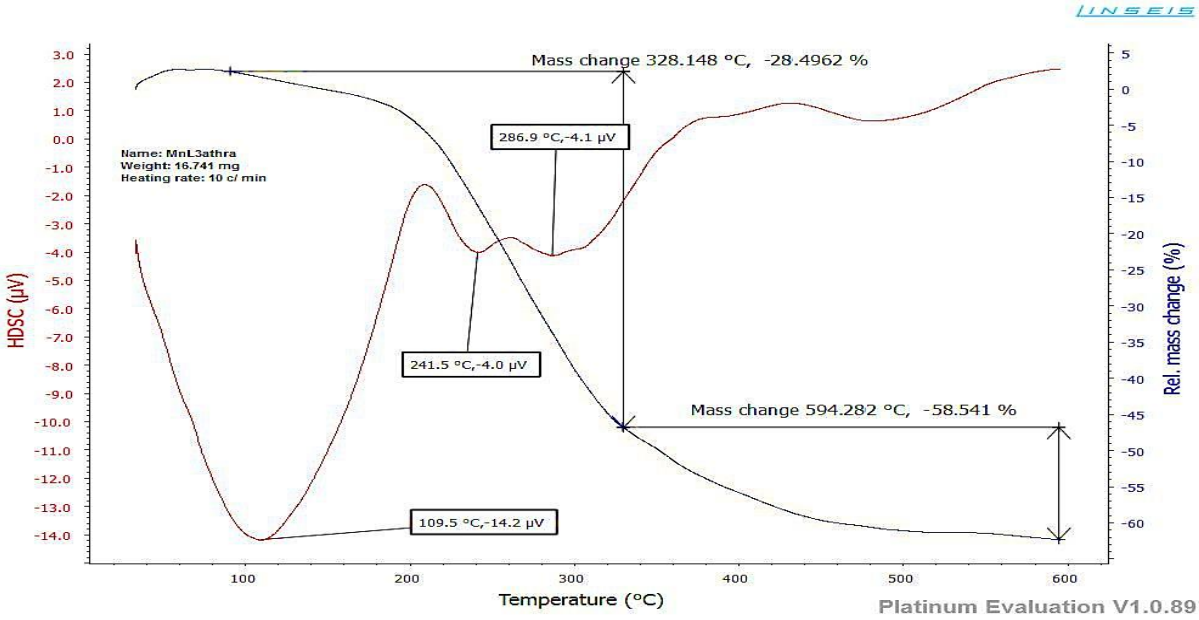

Figure 15. Thermogram of Manganese-complex

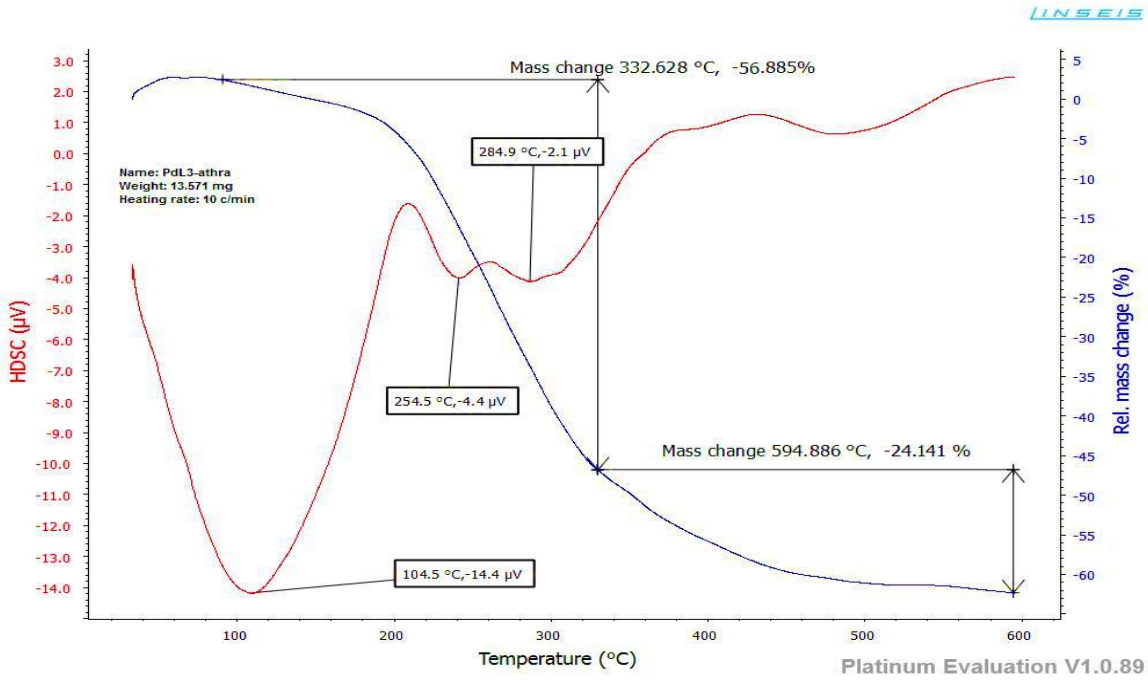

Figure 16. Thermogram of Palladium-complex

2024, 21(6): 1960-1982
https://doi.org/10.21123/bsj.2023.8188
P-ISSN: 2078-8665 - E-ISSN: 2411-7986
Baghdad Science Journal

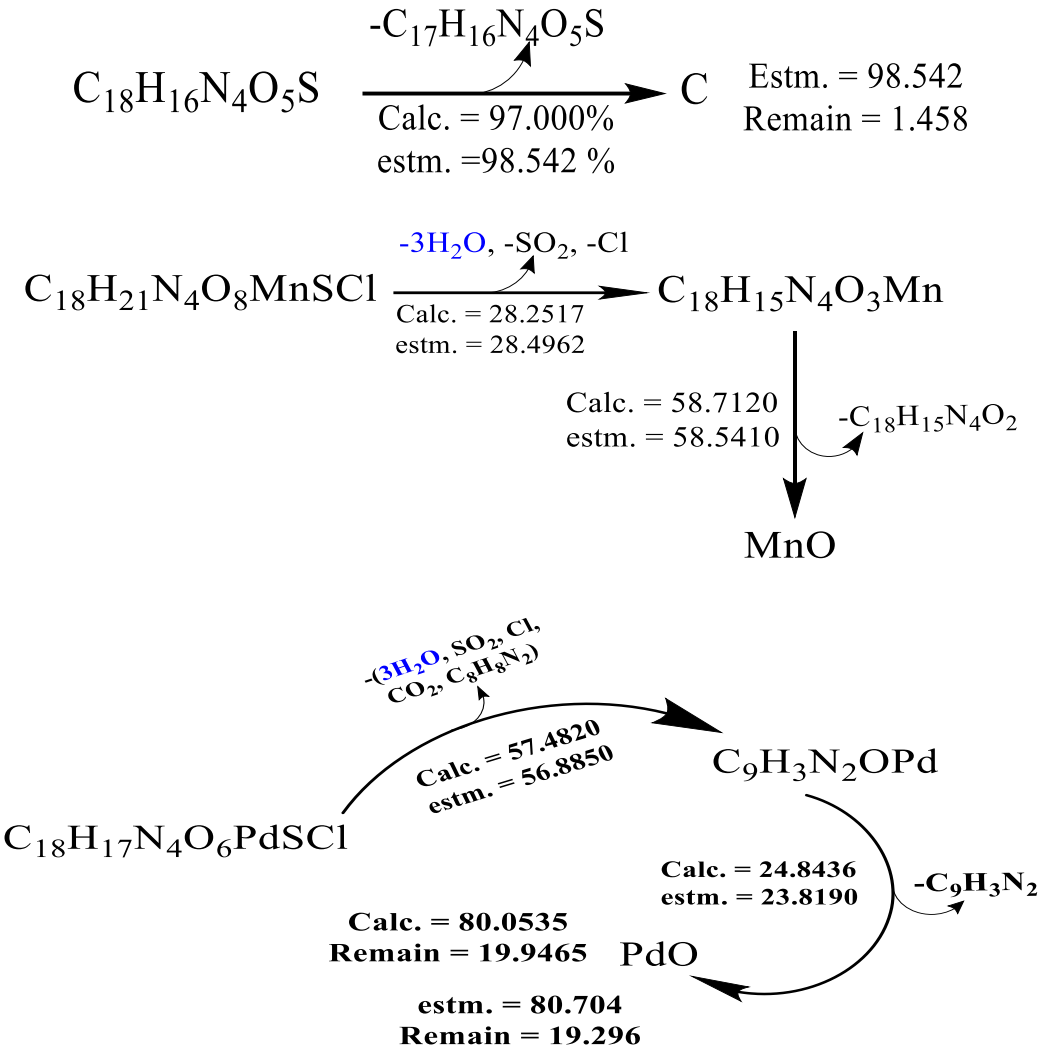

Scheme 8. Pyrolysis pathway of complexes

Table 7. DSC records of ligand (HL) and some complexes

Compound	T_i / °C	T_f/ °C	ΔH J/g	Max temp.˚C and Type
$C_{18}H_{16}N_4O_5S$	47	596	-12.4 -7.6 -9.8	95.4 endo. 200.1 endo. 309.9 endo.
$C_{18}H_{21}ClMnN_4O_8S$	92 328.148	328.148 594.282	-14.2 - 4.0	109.5- endo. 241.5- endo. 286.9- endo.
$C_{18}H_{17}N_4PdO_6SCl$	92 332.628	332.628 594.886	-14.4 -4.4 -2.1	104.5- endo. 254.5- endo. 284.9- endo.

2024, 21(6): 1960-1982
https://doi.org/10.21123/bsj.2023.8188
P-ISSN: 2078-8665 - E-ISSN: 2411-7986
Baghdad Science Journal

Table 8. TGA data of ligand (HL) and some complexes

Compound	T_i / °C	T_f/ °C	$T_{DTG\ max}$	% Estimated (calc.) Mass loss	Total mass loss	Assignment
$C_{18}H_{16}N_4O_5S$	47	596	320	98.542 (96.683)	98.542 (96.683)	$-C_{17}H_{16}N_4O_5S$
Calculated: 97.000% final = 3.000%; Estimated 98.542% final = 1.458%						
$C_{18}H_{21}ClMnN_4O_8S$	92	328.148	190	28.4962 (28.2517)	86.540 (87.037)	$-3H_2O$ $-SO_2$, -Cl
	328.148	594.282	440	58.5410 (58.7120)		$-C_{18}H_{15}N_4O_3$ MnO
Calculated: 87.037% final = 12.963%; Estimated 86.540% final = 13.46%						
$C_{18}H_{17}N_4PdO_6SCl$	92	332.628	190	56.8850 (57.4820)	80.053 (80.704)	$-3H_2O$, $-C_8H_8N_2$ -Cl, $-CO_2$, $-SO_2$
	166.495	241.841	200	23.8190 (24.8436)		$-C_9H_3N_2$ PdO
Calculated: 80.704% final =19.296%;Estimated 80.053% final =19.947%						

Diagnosis of Antioxidant Activity

The reduction of DPPH radical intensity in this work is due to the interaction of the complexes with radical and, as such, scavenging the radicals by hydrogen donation, as shown in Table 9. The DPPH activities by the complexes displayed robust electron-donating power compared with the azo-ligand. Fig. 17 exhibited higher activity against DPPH than the commercially available Ligand HL; however, the values in the existence of PdL as metal showed the highest activity compared with the rest of complexes and ligand. This is due to the coordination and hydrogen-donor of the hydroxyl groups and occupied orbitals in metal ions. The order of our compounds follow as:

(GA>[Pd(L)(H_2O)Cl]>[Fe(L)(H_2O)$_2$$Cl_2$]>[Mn(L)($H_2O$)$_3$Cl]>[Cr(L)($H_2O$)$_2$$Cl_2$]>HL) [41-44].

Pd-Complex has the higher antioxidant activity because of its highest positive charge among the prepared compounds which can completely inhibit the activity of free radicals

2024, 21(6): 1960-1982
https://doi.org/10.21123/bsj.2023.8188
P-ISSN: 2078-8665 - E-ISSN: 2411-7986
Baghdad Science Journal

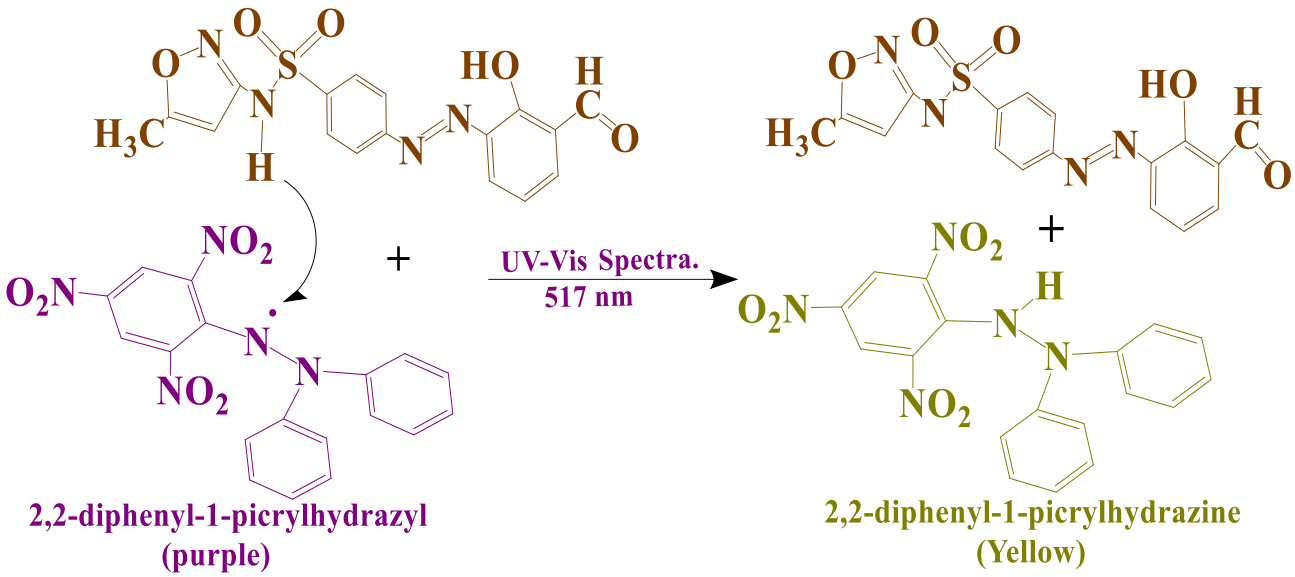

Scheme 9. Conversion of DPPH (purple) to its corresponding hydrazine form (yellow) by the addition of (Ligand HL) compounds to DPPH due to proton transfer

Table 9. Inhibitory action data of ligand (HL) and its minerals

Compounds	Mean	Standard deviation	Coefficient of variation %	Correlation coefficient	IC_{50} (M) DPPH
GA	94.362	1.983215	1.835768	0.996754	-6.3327
HL	79.379	5.968351	5.134078	0.983765	2.6653
$C_{18}H_{21}ClMnN_4O_8S$	59.634	25.377681	21.771663	0.991063	0.476
$C_{18}H_{17}N_4PdO_6SCl$	3.216	3.217787	5.321768	0.963277	-2.0016
$C_{18}H_{19}Cl_2FeN_4O_7S$	52.376	9.766608	42.078354	0.997836	0.471
$C_{18}H_{19}Cl_2CrN_4O_7S$	39.318	23.332462	42.662501	0.993267	0.488

Note: IC_{50}: the half-maximal inhibitory concentration

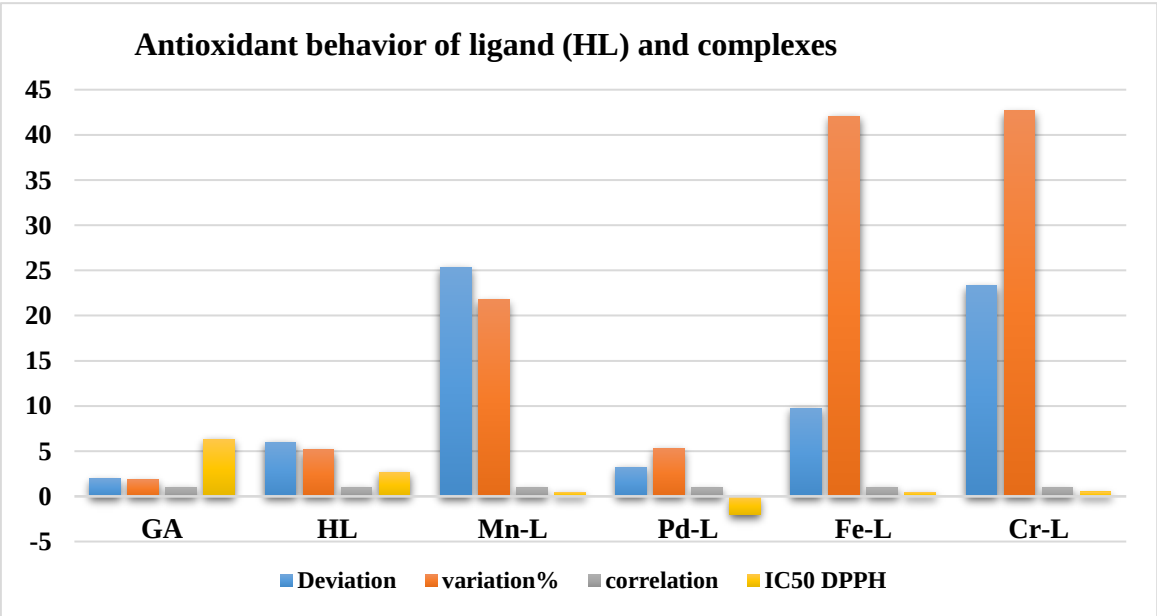

Figure 17. Inhibitory action of ligand HL and its minerals

Conclusion

In conclusion, we have prepared Azo Dye 4-((3-formyl-2-hydroxyphenyl)diazenyl)-N-(5-methylisoxazol-3-yl)benzenesulfonamide and its complexes. All the prepared complexes possessed an octahedral geometry but square planer for Pd(II) which confirmed via Uv-Vis, mass spectroscopy. Therefore, the spectroscopic investigation of all complexes has indicated that the ligand HL is bidentate ligand and it is coordinated with the metal ions through N.O atoms. The compounds showed outstanding radical scavenging activities against super oxide anion radical, nitric oxide radical, DPPH radical and hydrogen peroxide. Of all these targeted compounds ($[Pd(L)(H_2O)Cl]$, $[Fe(L)(H_2O)_2Cl_2]$, $[Mn(L)(H_2O)_3Cl]$ and $[Cr(L)(H_2O)_2Cl_2]$ showed better antioxidant activity than Gallic acid ligand in DPPH assay. The values in the existence of methanol and chloroform showed the highest activity compared of all studied solvents. Based on the result, it is clear that these complexes can be used as good antioxidants in the field of food industry and medicinal.

Authors' Declaration

- Conflicts of Interest: None.
- We hereby confirm that all the Figures and Tables in the manuscript are ours. Furthermore, any Figures and images, that are not ours, have been included with the necessary permission for re-publication, which is attached to the manuscript.
- Ethical Clearance: The project was approved by the local ethical committee at University of Baghdad.

Authors' Contribution Statement

A. G. A. Conducted the practical side of the research, analysis of the results, and the writing of the manuscript. A. A. S. conceived the idea of the research, contributed in the analysis of the results and did the revision and the proofreading of the manuscript.

References

1. Ibraheem IH, Mubder NS, Abdullah MM,Al-Neshmi H. Synthesis, characterization and bioactivity Study from azo–ligand derived frommethyl-2-amino benzoatewith some metal ions. Baghdad Sci J. 2022; 0114-0114. http://dx.doi.org/10.21123/bsj.2022.6584
2. Wannas N.M., Al-Hamdani A.A.S., Al-Zoubi W., Spectroscopic characterization for new complexes with 2,2'- (5,5-dimethylcyclohexane-1,3-diylidene)bis(azan-1-yl- 1-ylidene) dibenzoic acid, JPOC, 2020, 33:e4099. https://doi.org/10.1002/poc.4099
3. Malik H, Akhter Z, Shahbaz M, Yousuf S, Munawar KS, Muhammad S, et al. Synthesis, spectroscopic characterization, single crystal, theoretical investigation, and biological screenings of azo-based moieties. J Mol Struct. 2022; 1270: 133867.https://doi.org/10.1016/j.molstruc.2022.133867
4. Nagasundaram N, Govindhan C, Sumitha S, Sedhu N, Raguvaran K, Santhosh S, et al. Synthesis, characterization and biological evaluation of novel azo fused 2, 3-dihydro-1H-perimidine derivatives: In vitro antibacterial, antibiofilm, anti-quorum sensing, DFT, in silico ADME and Molecular docking studies. J Mol Struct. 2022; 1248: 131437.https://doi.org/10.1016/j.molstruc.2021.131437
5. Hamad SF, Ibraheem TK. Synthesis, Characterize and Antibacterial Evaluate of Some Novel Compounds Containing 1, 3, 4-thiadiazole. J Pharm Negat. 2022; 1119-1122.https://doi.org/10.47750/pnr.2022.13.S03.176
6. Mir MA, Ashraf MW. Synthesis, Characterization and Biochemical Analysis of Azo-metal complex of Embelin with Second Group Transition Metals. Curr Organocatalysis. 2022; 9(2): 155-162. https://doi.org/10.2174/2213337208666211102104240
7. Turan N, Buldurun K. Synthesis, characterization and antioxidant activity of Schiff base and its metal complexes with Fe (II), Mn (II), Zn (II), and Ru (II) ions: Catalytic activity of ruthenium (II) complex.

Eur J Chem. 2018; 9(1): 22-29. https://doi.org/10.5155/eurjchem.9.1.22-29.1671
8. Mohammed H. Synthesis, Identification, and Biological Study for Some Complexes of Azo Dye Having Theophylline. Sci world J. 2021 Jul 22; 2021. https://doi.org/10.1155/2021/9943763
9. Ispir E, Ikiz M, Inan A, Sünbül AB, Tayhan SE, Bilgin S, et al. Synthesis, structural characterization, electrochemical, photoluminescence, antiproliferative and antioxidant properties of Co (II), Cu (II) and Zn (II) complexes bearing the azo-azomethine ligands. J Mol Struct. 2019 Apr 15; 1182: 63-71. https://doi.org/10.1016/j.molstruc.2019.01.029
10. El-Zomrawy AA. Selective and sensitive spectrophotometric method to determine trace amounts of copper metal ions using Amaranth food dye Spectrochim. Acta - A: Mol. Biomol. Spectrosc. 2018 Oct 5; 203: 450-4. https://doi.org/10.1016/j.saa.2018.06.014
11. Kareem MJ, Al-Hamdani AAS, Young GK, Al-Zoubi W, Saad GM. Synthesis, characterization,Anddetermination antioxidant activities for new Schiffbase complexes derived from 2-(1H-indol-3-yl)-ethylamine and metal ion complexes. J Mol Struc.2021 May; 1231:129669. https://www.iasj.net/iasj/article/101293
12. Kyei SK, Akaranta O, Darko G. Synthesis, characterization and antimicrobial activity of peanut skin extract-azo-compounds. Sci Afr. 2020 Jul 1; 8: e00406. https://doi.org/10.1016/j.sciaf.2020.e00406
13. Mahdy AR, Ali OA, Serag WM, Fayad E, Elshaarawy RF, Gad EM. Synthesis, characterization, and biological activity of Co (II) and Zn (II) complexes of imidazoles-based azo-functionalized Schiff bases. J Mol Struct. 2022 Jul 5; 1259: 132726. https://doi.org/10.1016/j.molstruc.2022.132726
14. Kyhoiesh HA, Al-Adilee KJ. Synthesis, spectral characterization, antimicrobial evaluation studies and cytotoxic activity of some transition metal complexes with tridentate (N, N, O) donor azo dye ligand. Results Phys. 2021 Jan 1; 3: 100245. https://doi.org/10.1016/j.rechem.2021.100245
15. Mandour HS, Abouel-Enein SA, Morsi RM, Khorshed LA. Azo ligand as new corrosion inhibitor for copper metal: Spectral, thermal studies and electrical conductivity of its novel transition metal complexes. J Mol Struct. 2021 Feb 5; 1225: 129159. https://doi.org/10.1016/j.molstruc.2020.129159
16. Minnelli C, Laudadio E, Galeazzi R, Rusciano D, Armeni T, Stipa P, et al. Synthesis, characterization and antioxidant properties of a new lipophilic derivative of edaravone. Antioxidants. 2019; 8(8): 258. https://doi.org/10.3390/antiox8080258
17. Bingöl M, Turan N. Schiff base and metal (II) complexes containing thiophene-3-carboxylate: Synthesis, characterization and antioxidant activities. J Mol Struct. (2020); 1205: 127542.https://doi.org/10.1016/j.molstruc.2019.127542
18. Abdulrazzaq AG, Al-Hamdani A A S.Some Metal Ions Complexes With Azo [4-((8-hydroxyquinolin-7-yl)-N(4methylisoxazol3yl)benzenesulfonamide Synthesis, Characterization, Thermal Study and Antioxidant Activity. J. Med. Chem.Sci.2022; 6(2): 236-249. https://doi.org/10.26655/JMCHEMSCI.2023.2.7
19. Masoud MS, Sweyllam AM, Ahmed MM. Synthesis, characterization, coordination chemistry and biological activity of some pyrimidine complexes. J Mol Struct. 2020; 1219: 128612.https://doi.org/10.1016/j.molstruc.2020.128612
20. Al-Atbi HS, Al-Salami BK, Al-Assadi IJ. New azo-azomethine derivative of sulfanilamide: Synthesis, Characterization, Spectroscopic, Antimicrobial and Antioxidant activity study. J Phys Conf. 2019; 1294 (5): 052033. https://doi.org/10.1088/1742-6596/1294/5/052033
21. Mahdi MA, Jasim LS, Mohamed MH. Synthesis, Spectral and Biological Studies of Co (II), Ni (II) and Cu (II) Complexes with New Heterocyclic Ligand Derived From Azo-Dye. Syst Rev Pharm. 2021 Feb 1; 12: 426-34.https://doi.org/10.1080/00958970802226387
22. Witwit IN, Farhan HM, Motaweq ZY. Preparation of Mixed ligand Complexes of Heterocyclic AzoQuinoline Ligand and Imidazole Molecule with Some of Divalent Transition Ions and their Biological Activity Against Multi Drug Resistance Pathogenic Bacteria. J Phys Conf Ser. 2021 ; 1879(2) : 022064. https://doi.org/10.1088/1742-6596/1879/2/022064
23. Rahman M, Haque TM, Sourav NS, Rahman S, Yesmin S, Mia R, et al. Synthesis and investigation of dyeing properties of 8-hydroxyquinoline-based azo dyes. J Iran Chem Soc. 2021 Apr; 18(4): 817-26.https://doi.org/10.1007/s13738-020-02070-2
24. Al-Zoubi W, Kim MJ, Yoon DK, Al-Hamdani AAS, Kim YG, Young GK. Effect of organiccompounds and rough inorganic layer formed by plasma electrolytic oxidation on photocatalyticperformance. J Alloys Compd.2020 May 15;823: 153787. https://doi.org/10.1002/poc.4099
25. Mohammed HS, Al-Hasan HA, Chaieb Z, Zizi Z, Abed HN. Synthesis, characterization, DFT calculations and biological evaluation of azo dye ligand containing 1, 3-dimethylxanthine and its Co (II), Cu (II) and Zn (II) complexes. Bull Chem Soc

Ethiop.2023; 37(2); 347-356. https://doi.org/10.4314/bcse.v37i2.8
26. Unnisa A, Abouzied AS, Baratam A, Lakshmi KC, Hussain T, Kunduru RD, Selvarajan KK. Design, synthesis, characterization, computational study and in-vitro antioxidant and anti-inflammatory activities of few novel 6-aryl substituted pyrimidine azo dyes. Arab J Chem. 2020; 13(12): 8638-8649.https://doi.org/10.1016/j.arabjc.2020.09.050
27. uleman VT, Al-Hamdani AAS, Ahmed SD, Jirjees VY, Khan ME, Dib A, Al Zoubi W, KoYG. Phosphorus Schiff base ligand and its complexes: Experimental and (https://onlinelibrary.wiley.com/doi/abs/10.1002/aoc.5546) theoretical investigations (https://onlinelibrary.wiley.com/doi/abs/10.1002/aoc.5546). Appl. Organomet. Chem., 2020;(34)4; e5546. https://doi.org/10.1002/aoc.5546
28. Zayed EM, Mohamed GG, Abd El Salam HA. Ni (II), Co (II), Fe (III), and Zn (II) mixed ligand complexes of indoline-dione and naphthalene-dione: Synthesis, characterization, thermal, antimicrobial, and molecular modeling studies. Inorg Chem Commun. 2023; 147: 110276.https://doi.org/10.1016/j.inoche.2022.110276
29. Moamen SR, Altalhi T , Safyah BB, Ghaferah HA, Kehkashan A. New Cr(III), Mn(II), Fe(III), Co(II), Ni(II), Zn(II), Cd(II),and Hg(II) Gibberellate Complexes: Synthesis, Structure,and Inhibitory Activity Against COVID-19 Protease. Russ J Gen Chem. 2021; 91(5): 890–896. https://doi.org/10.1134/S1070363221050194
30. Kyei SK, Akaranta O, Darko G. Synthesis, characterization and antimicrobial activity of peanut skin extract-azo-compounds. Sci Afr. 2020; 8: e00406.https://doi.org/10.1016/j.sciaf.2020.e00406
31. Maliyappa MR, Keshavayya J, Mallikarjuna NM, Krishna PM, Shivakumara N, Sandeep T, et al. Synthesis, characterization, pharmacological and computational studies of 4, 5, 6, 7-tetrahydro-1, 3-benzothiazole incorporated azo dyes. J Mol Struct. 2019; 1179: 630-641.https://doi.org/10.1016/j.molstruc.2018.11.041
32. Al-Daffay RK, Al-Hamdani AA. Synthesis, Characterization, and Thermal Analysis of a New Acidicazo Ligand's Metal Complexes. Baghdad Sci J. 2022; 19(3): 121-33. : http://dx.doi.org/10.21123/bsj.2022.6709
33. Mallikarjuna NM, Keshavayya J, Maliyappa MR, Ali RS, Venkatesh T. Synthesis, characterization, thermal and biological evaluation of Cu (II), Co (II) and Ni (II) complexes of azo dye ligand containing sulfamethaxazole moiety. J Mol Struct. 2018; 1165: 28-36.https://doi.org/10.1016/j.molstruc.2018.03.094
34. Waheeb AS, Al-Adilee KJ. Synthesis, characterization and antimicrobial activity studies of new heterocyclic azo dye derived from 2-amino-4, 5-dimethyl thiazole with some metal ions. Mater Today: Proc. 2021; 42: 2150-2163.https://doi.org/10.1016/j.matpr.2020.12.299
35. Turan N, Buldurun K. Synthesis, characterization and antioxidant activity of Schiff base and its metal complexes with Fe (II), Mn (II), Zn (II), and Ru (II) ions: Catalytic activity of ruthenium (II) complex. Eur J Chem. 2018 Mar 31; 9(1): 22-9. https://doi.org/10.5155/eurjchem.9.1.22-29.1671 |
36. Omidi S, Khojasteh V, Kakanejadifard A, Ghasemian M, Azarbani F. Synthesis, characterization, spectroscopy and biological activity of 4-((3-formyl-4-hydroxyphenyl) azo)-1-alkylpyridinium salts. Chem Sci J. 2018; 130(8): 1-9. https://doi.org/10.1007/s12039-018-1521-5
37. EL-Gammal OA, Alshater H, El-Boraey HA. Schiff base metal complexes of 4-methyl-1H-indol-3-carbaldehyde derivative as a series of potential antioxidants and antimicrobial: Synthesis, spectroscopic characterization and 3D molecular modeling. J Mol Struct. 2019 Nov 5; 1195: 220-30. https://doi.org/10.1016/j.molstruc.2019.05.101
38. Ahmad K, Naseem HA, Parveen S, Shah SSA, Shaheen S, Ashfaq A, et al. Synthesis and spectroscopic characterization of medicinal azo derivatives and metal complexes of Indandion. J Mol Struct. 2019; 1198: 126885.https://doi.org/10.1016/j.molstruc.2019.126885
39. Olesya S, Alexander P. Antimicrobial activity of mono-and polynuclear platinum and palladium complexes. Foods Raw Mater. 2020; 8(2): 298-311. http://doi.org/10.21603/2308-4057-2020-2-298-311
40. Abbas AK. Lanthanide ions complexes of 2-(4-amino antipyrine)-L-Tryptophane (AAT): preparation, Identification and antimicrobial assay. Iraqi J. Sci. 2015;56(4C):3297-09. https://doi.org/10.1108/PRT-01-2018-0005
41. Mihsen HH, Abass SK, Hassan ZM, Abass AK. Synthesis, Characterization and Antimicrobial Activities of Mixed Ligand Complexes of Fe (II), Co (II), Ni (II) and Cu (II) Ions Derived from Imine of Benzidine and o-phenylenediammine. Iraqi J Sci. 2020 Nov 28: 2762-75. https://doi.org/10.24996/ijs.2020.61.11.2
42. Kadhim SM, Mahdi SM. Preparation and Characterization of New (Halogenated Azo-Schiff) Ligands with Some of their Transition Metal Ions Complexes. Iraqi J Sci. 2022 Aug 31:3283-99. https://doi.org/10.24996/ijs.2022.63.8.4

43. Reda SM, Al-Hamdani AA. Mn (II), Fe (III), Co (II) and Rh (III) complexes with azo ligand: Synthesis, characterization, thermal analysis and bioactivity Baghdad Sci J. 2022. https://doi.org/10.21123/bsj.2022.7289

44. Al-Daffay RK, Al-Hamdani AA. Synthesis and Characterization of Some Metals Complexes with New Acidicazo Ligand 4-[(2-Amino-4-Phenylazo)-Methyl]-Cyclohexane Carboxylic Acid. Iraqi J Sci.. 2022 Aug 31:3264-75 https://doi.org/10.24996/ijs.2022.63.8.2

تحضير ، تشخيص ، دراسة التحلل الحراري و فعالية مضادات الاكسدة لمعقدات بعض ايونات معادن الكروم الثلاثي والحديد الثلاثي والمنغنيزالثنائي والبلاديوم الثنائي مع صبغة ازو مشتقة من بارا- مثل-2-هيدروكسي بنزلديهايد

عذراء غازي عبد الرزاق، عباس علي صالح الحمداني

قسم الكيمياء، كلية العلوم للبنات، جامعة بغداد، بغداد، العراق.

الخلاصة

ليكاند ازو جديد.,4-((3-formyl-2-hydroxyphenyl)diazenyl)-N-(5-methylisoxazol-3-yl)benzenesulfonamide اللليكاند المحضر استعمل لتحضير معقدات من ايونات معادن مختلفة مثل الكروم الثلاثي والمنغنيز الثنائي والحديد الثلاثي والبلاديوم الثنائي بنسب مولية (1:1) (ليكاند : فلز) نتائج التشخيص للمركبات بتقنيات مطيافية الاشعة فوق البنفسجية الاشعة تحت الحمراء الرنين النووي المغناطيسي البروتوني والكربوني وطيف الكتلة والتحليل الدقيق للعناصر ومحتوى الفلز والتوصيلية المولارية والحساسية المغناطيسية ومنحنى التحليل الحراري الوزني والتفاضلي، اعطت النتائج شكل ثماني السطوح لمعقدات الكروم والمنغنيز والحديد بينما اعطى مربع مستوي لمعقد البلاديوم. تم تقييم الانشطة المضادة للاكسدة للمركبات المحضرة باستخدام 1،1- ثنائي فنيل -2-بيكرل هايدرازول باعتباره الجذر الحر، واظهرت النتائج ان صبغة الازو ومعقداتها تمتلك نشاطاً قوياً مضاداً للاكسدة . تشير العلاقة بين التركيب والنشاط لليكاند ومعقداته الى ان وجود قابلية الوهب بالالكترون لمعقدات الكروم والمنغنيز والحديد في التركيب الكيميائي يزيد النشاط في حين ان معقد البلاديوم يقل نشاطه ضدة الاكسدة مما يشير الى تفوق جذر الهيدروكسيل على جذور الاكسدة.

الكلمات المفتاحية: مضادات الاكسدة, صبغة الازو , 2-هيدروكسي بنزالديهايد, مطيافية الكتلة, التحاليل الحرارية.